Neuergebnisse aus dem Paläozoikum der Ost- und Südalpen			. Redaktion: Hans Peter Schönlaub & Albert Daurer		
Jb. Geol. B.-A.	ISSN 0016-7800	Band **135**	Heft 1	S. 57-98	Wien, März 1992

The Devonian/Carboniferous Boundary in the Carnic Alps (Austria) – A Multidisciplinary Approach

By HANS P. SCHÖNLAUB, MOSES ATTREP, KLAUS BOECKELMANN, ROLAND DREESEN, RAIMUND FEIST, ALOIS FENNINGER, GERHARD HAHN, PETER KLEIN, DIETER KORN, ROLAND KRATZ, MORDECKAI MAGARITZ, CHARLES J. ORTH & JOSEF-MICHAEL SCHRAMM*)

With 21 Text-Figures, 3 Tables and 9 Plates

Austria
Carnic Alps
Devonian/Carboniferous Bundary
Conodonts
Ammonoids
Trilobites
Stable Isotopes
Geochemistry
Metamorphism

Österreichische Karte 1 : 50.000
Blatt 197

Contents

*) Authors' addresses: Univ.-Doz. Dr. HANS P. SCHÖNLAUB, Dr. PETER KLEIN, Geologische Bundesanstalt, P.O. Box 154, Rasumofskygasse 23, A-1031 Wien; Dr. MOSES ATTREP, Jr., Dr. CHARLES J. ORTH, Isotope and Nuclear Chemistry Division, Los Alamos National Laboratory, Los Alamos, N. M. 87545, USA; Dr. KLAUS BOECKELMANN, Institut für Geologie und Paläontologie, TU Berlin, Ernst-Reuter-Platz 1, D-1000 Berlin; Dr. ROLAND DREESEN, Institut Scientifique de Service Public, Rue du Chéra, 200, B-4000 Liège, Belgique; Dr. RAIMUND FEIST, Laboratoire de Paléontologie, U.S.T.L., Place E. Bataillon, F-34060 Montpellier, France; Univ.-Prof. Dr. ALOIS FENNINGER, Institut für Geologie und Paläontologie, Universität, Heinrichstraße 26, A-8010 Graz; DIETER KORN, Institut für Geologie und Paläontologie, Universität, Sigwartstraße 10, D-7400 Tübingen; Univ.-Prof. Dr. GERHARD HAHN, Dipl.-Geol. ROLAND KRATZ, Institut für Geologie und Paläontologie, Universität, Fachbereich 18, Lahnberge, Hans-Meerwein-Straße, D-3550 Marburg; Dr. MORDECKAI MAGARITZ, Environmental Science and Energy Research, The Weizmann Institute of Science, 76100 Rehovot, Israel; Univ.-Prof. Dr. JOSEF-MICHAEL SCHRAMM, Institut für Geologie und Paläontologie, Universität, Hellbrunner Straße 34/III, A-5020 Salzburg.

Die Devon/Karbon-Grenze in den Karnischen Alpen (Österreich) – Eine Fallstudie interdisziplinärer Zusammenarbeit

Zusammenfassung

Die vorliegende Arbeit ist eine ausführliche Zusammenfassung von erweiterten und neuen Ergebnissen von Einzelarbeiten zum Geschehen an der Devon/Karbon-Grenze in den Profilen Grüne Schneid und Kronhofgraben der zentralen Karnischen Alpen. Ersteres ist durch kontinuierliche Karbonatsedimentation an der Wende vom Devon zum Karbon gekennzeichnet. Eine reiche Conodonten-, Clymenien- und Goniatiten- sowie Trilobitenführung ermöglichen die exakte Festlegung des Grenzniveaus im oberen Teil der Kalkbank 6 (26.5 cm über der Basis von Bank 6) sowie eine Feingliederung in einzelne Zonen mit entsprechenden Leitformen von Conodonten, Ammonoideen und Trilobiten. Wechselnde Verhältnisse von Fazies-abhängigen Conodontenassoziationen und der vertikale Wechsel zwischen blinden und nicht-blinden Trilobiten sind Hinweise für geringfügige Meeresspiegelschwankungen im jüngsten Oberdevon und in der älteren Tournais-Stufe. Kurz vor Ende des Oberdevons (Mittlere praesulcata-Zone) kommt es als Folge des „Hangenberg-Events" zu einer Regression, die in der duplicata Zone des älteren Tournai von einem Meeresspiegelanstieg gefolgt wird.

Die umfangreichen biostratigraphischen Untersuchungen werden ergänzt von lithofaziellen, mineralogischen, geochemischen und isotopenchemischen Analysen. Aus der Fülle von Daten schließen wir, daß im Profil Grüne Schneid – wie bisher von keiner anderen Stelle auf der Erde mit dieser Exaktheit nachgewiesen – über die Devon/Karbon-Grenze hinweg ununterbrochen und in gleichbleibender Fazies Kalksedimentation stattfand. Hinweise auf Hartgründe, Schichtlücken und Umlagerungen fehlen ebenso wie jegliche Hinweise auf ein extraterrestrisches Ereignis. Diese Erkenntnisse sowie die „drittrangige" Bedeutung der Grenze in Hinblick auf ein Massensterben unterstreichen die Auffassung, das Profil Grüne Schneid als weltweit geeignetes Referenzprofil für die Grenze Devon/Karbon erneut vorzuschlagen.

Im 9 km entfernten D/C-Profil des Kronhofgrabens schaltet sich an der Devon/Karbon-Grenze ein 50 cm mächtiger pyritreicher Schieferhorizont in die Kalkabfolge ein. Sein Chemismus weist erhöhte Gehalte von organischem Kohlenstoff, Schwefelkies, Iridium und von Schwermetallen auf. Für die Bildung dieses Äquivalents der „Hangenberg-Schwarz-Schiefer" des Rheinischen Schiefergebirges wird ein reduzierendes Milieu vermutet. Lithofazies, Conodonten und blinde Trilobiten sind darüberhinaus Hinweise auf einen im Vergleich zur Lokalität Grüne Schneid tieferen Bildungsraum. Als Ursache wird eine lokal verstärkte Subsidenz angenommen, die die Regressions-Transgressionstendenz im flacheren Grüne-Schneid-Areal überlagert.

Abstract

This paper presents new and revised sedimentological, paleontological, geochemical and isotopic data on two D/C boundary sections from the Carnic Alps of southern Austria, the Grüne Schneid and the Kronhofgraben sections. Based on rich abundances of conodonts, ammonoids and trilobites for the Grüne Schneid section continuous and uniform sedimentation is concluded across the boundary. The D/C boundary lies within the upper part of the 32 cm thick limestone bed no. 6, and more precisely 26.5 cm above its base. In succcessive order different associations of conodonts, ammonoids and trilobites have been recognized in the studied 6 m thick section. Of particular interest are the varying abundances of facies-related conodont genera and the occurrences of blind and oculated trilobites. Comprehensive geochemical and isotopic analysis support the conclusion of an uninterrupted sequence. In addition, there is no indication suggesting an extraterrestrial component in the sediment nor is there a strong argument for a severe mass mortality. Rather, the available information suggests a moderate regressive event shortly before the end of the Devonian, followed by a transgression at the beginning of the duplicata Zone of early Tournaisian age.

As a consequence, Grüne Schneid section is regarded to serve as the excellent stratotype for the D/C boundary. It fulfills all criteria required for a reference section, such as abundances of various fossil groups, continuity and uniformity of facies. The total absence of hardgrounds, stratigraphic gaps or reworking further supports this recommendation although the D/C boundary matter seems to have settled more recently.

The Kronhofgraben section, located some 9 km to the east of the Grüne Schneid section, is characterized by a 50 cm thick shale intercalation in the overall limestone succession. In comparison with the area of Grüne Schneid it represents a deeper environment. This conclusion is reached from analysis of the facies and the fauna such as conodonts and trilobites. In the shale horizon the contents of organic carbon, sulfur, heavy metals and of Ir are considerably enriched, suggesting deposition under reduced stagnant conditions below the maximum carbonate sedimentation depth. Presumably the metal enrichments were caused by oceanic processes and not from cosmic dust. Similar to the Grüne Schneid section the carbon isotope profile across the boundary interval shows no significant variations, which support the idea that no severe mass extinction occurred at or close to the D/C boundary, i.e. some 353 Ma ago.

1. Introduction

The Devonian/Carboniferous (D/C) boundary event, known also as "Hangenberg Event", has been widely recognized for a long time. It represents a significant although not major extinction event (Text-Fig. 1) that affected many pelagic organisms such as conodonts, ammonoids and trilobites and to a lesser extent also ostracodes, foraminifera and corals. Whether earth originated causes – tectonic, eustatic and volcanic – or extraterrestrial ones can be held responsible for this turnover has been variously speculated in recent times.

Recently, based on zircon crystal age data using the SHRIMP ion microprobe, statistically indistinguishable ages of 353.2 ± 4.0 Ma and 355.8 ± 5.6 Ma have been reported for bentonites lying 35 and 53 cm above the D/C boundary at Hasselbach, Germany, and Glenbawn, Australia, respectively. Consequently, for the "Hangen-

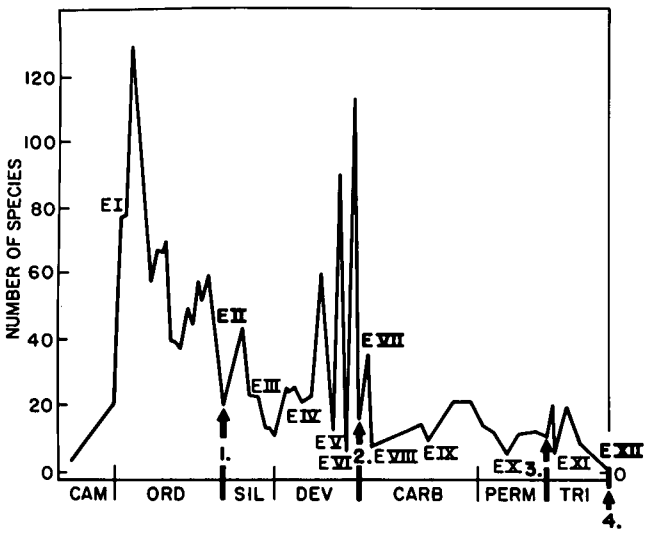

Text-Fig. 1.
Total number of conodont species appearing and major extinction events. 1,2,3,4 = times of extinction for other groups of organisms; EI to EXII = times of extinction for conodont species.
After D.L. CLARK, unpubl.

berg Event" an age of about 353 Ma may be estimated (G. YOUNG & J. CLAOUÉ-LONG, 1991). As will be shown here this event occurred shortly before the D/C boundary.

In the Carnic Alps of southern Austria and northern Italy the Devonian/Carboniferous boundary beds are excellently exposed. In a recent publication H.P. SCHÖNLAUB et al. (1991, Tab. 1, Text-Fig. 2) summarized the stratigraphic data from more than 20 limestone sections in which a continuous sedimentation across the Devonian/Carboniferous boundary has well been documented. At the end of the following stage, i.e., the Tournaisian, a drop in sea-level resulted in a karstification event which caused an extensive relief with limestone dissolution at surface and subsurface levels and local formation of fissures, caves and breccias (H.P. SCHÖNLAUB et al., 1991).

Since the official organisation of the IUGS Working Group on the Devonian/Carboniferous Boundary in 1976, many accomplishments were made towards a more accurate definition of the base of the Carboniferous Period. The level finally chosen in 1979 "represents an attempt at closest possible conformity with the current definition of the boundary, namely at the base of the Gattendorfia Zone as recommended by the 1935 Heerlen Congress" (E. PAPROTH, 1980). In 1979 it was generally agreed upon that this is at the first appearance of the conodont species *Siphonodella sulcata* within the evolutionary lineage from *S. praesulcata* to *S. sulcata*. Apparently this level is just below the entry (= lowermost record) of the ammonoid genus *Gattendorfia* in the Hönnetal section of the Rhenish massif.

Since then search began for the section best suited as boundary stratotype (see E. PAPROTH & M. STREEL (eds.), 1984; E. PAPROTH & G. D. SEVASTOPULO, 1988). Following the "Last call for candidate stratotypes" of 1985, in addition to three already existing candidate sections (Muhua, Berchogur, Hasselbachtal) four other sections were proposed to serve as stratotypes in 1987, namely Nanbiancun in southern China, Drewer in Germany, Grüne Schneid in the Carnic Alps of southern Austria and La Serre in the Montagne Noire, France. After lengthy discussion during the Courtmacsherry meeting in southern Ireland the latter gained the majority of support. Finally, in 1990 La Serre section was officially ratified by IUGS as Boundary Stratotype for the base of the Carboniferous.

Yet, by that time many specialists reached a broad consensus that in fact the Grüne Schneid section represents the best section of the marine realm as it contains rich assemblages of conodonts, ammonoids and trilobites of a high correlative potential. In addition, its succession displays a uniform lithology of cephalopod limestones suggesting the same distinct facies pattern for the latest Devonian and the earliest Carboniferous. The absence of any shaly intercalations, of gaps and/or reworked faunas or rocks may further indicate that the so-called "Hangenberg Event" did not affect the Grüne Schneid section. However, as will be shown for the Kronhofgraben section, this event can be recognized in other parts of the Carnic Alps. It reflects the culmination of a worldwide occurring regression followed by a transgression which on a global scale characterizes the D/C boundary.

This summary report presents new and updated results for the Devonian/Carboniferous boundary interval of the Carnic Alps (H.P. SCHÖNLAUB, 1969a; H.P. SCHÖNLAUB et al., 1988). This area which has long been famous for its almost uninterrupted fossiliferous sequences ranging from the Late Ordovician to Middle Triassic times seems to fulfill all requirements aimed at by the "Guidelines of the IUGS Commission on Stratigraphy" (J.W. COWIE et al., 1986). Its particular merits and peculiarities will be presented in the following chapters. Previous activities of research were extensively reviewed by H.P. SCHÖNLAUB et al. (1988) and H.P. SCHÖNLAUB et al. (1991).

2. Grüne Schneid Section

In the Central Carnic Alps, i.e. the area around Plöckenpaß (= Monte Croce Carnico) south of Kötschach-Mauthen the Variscan sequence is best exposed and stratigraphically continuous. Minor breaks, however, do occur locally, e.g., at the base of the Silurian, in the Middle Devonian and in the basal Frasnian. H.R. v. GAERTNER (1931) first concluded a conformity between the late Devonian and the Lower Carboniferous based on goniatites which he found in the uppermost limestone beds on top of the famous Cellon section. This locality is named "Grüne Schneid" (= "Green Crest" or "Cresta Verde"; Text-Fig. 2).

The Grüne Schneid section is located at an altitude of 2142 m on the Austrian, i.e., northern side of the crest forming the Austrian/Italian border some 25 meters west of the marker point n-129 which is west of the peak of mountain Cellon. It is easily accessible along the paths numbered 146 and 147 running from the pass to the top of the Cellon on the Italian side of the mountain chain.

The overall 6 m thick section displays the uppermost limestone beds of a 750 m thick conformable limestone sequence ranging from the Upper Ordovician to the Lower Carboniferous. The basal Tournaisian strata are separated from the overlying clastic Hochwipfel Formation by a fault zone.

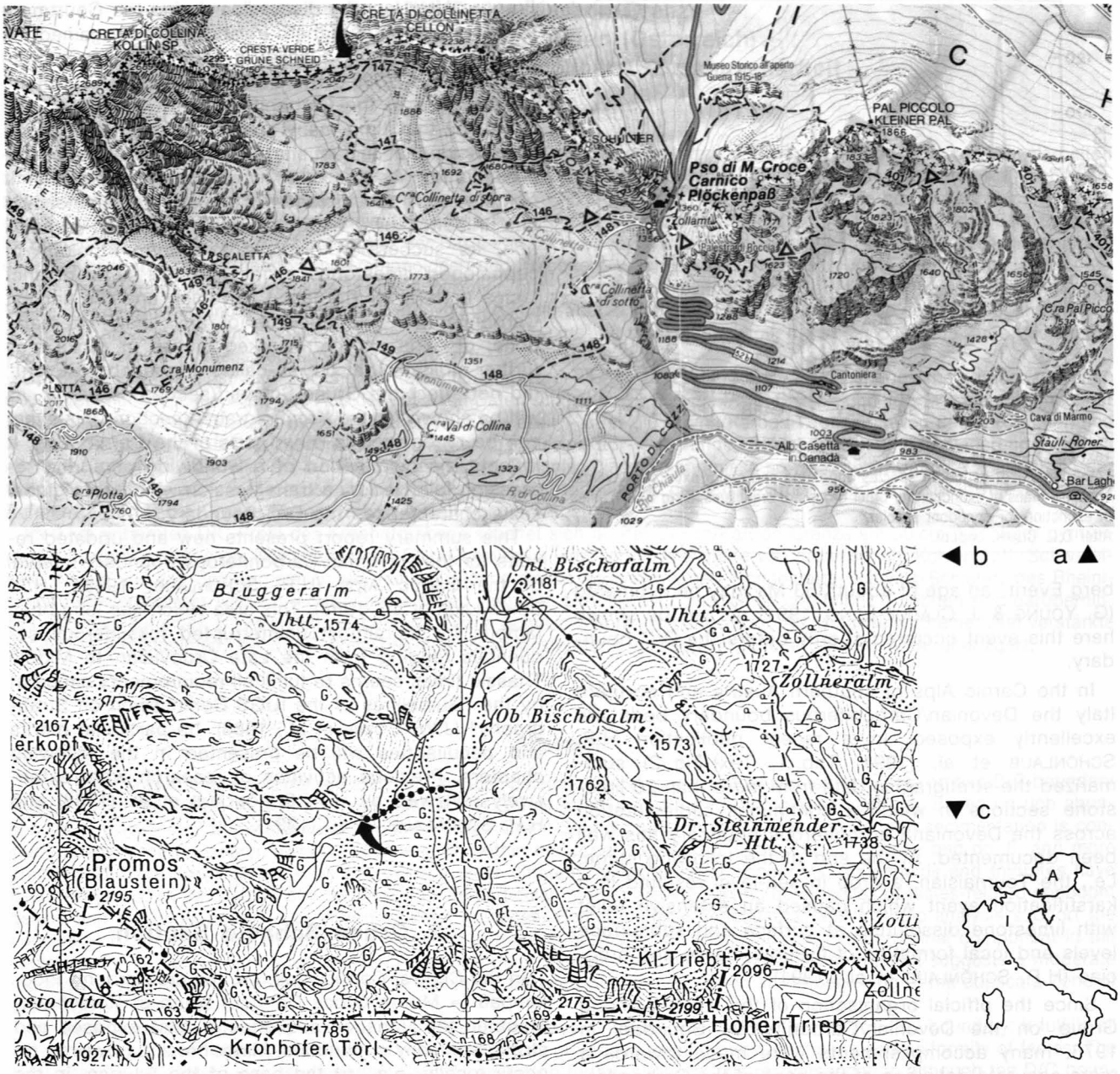

Text-Fig. 2.
Location of the study area in the Central Carnic Alps of Southern Austria.
A: Grüne Schneid section.
Topography after Carta Topografica per escursionisti 1 : 25.000, Foglio 09, Tabacco, Casa Editrice, Udine.
Actual scale ≈ 1 : 30.000.
B: Kronhofgraben section, 9 km east of Plöckenpaß.
Topography after ÖK 197 Kötschach 1 : 25.000, Bundesamt f. Eich- und Vermessungswesen, Wien.
Actual scale ≈ 1 : 30.000.
C: Approximate position at the Austrian/Italian border.

Recently the Cellon area was re-mapped (H.P. SCHÖNLAUB, 1985) and the outcrop was cleaned and enlarged. Now it exhibits a small cavern in the Devonian part and an excellently exposed bedded wall-rock in the boundary interval. The Tournaisian part of the section is 100 cm thick (Figs. 3 A,B, 4).

2.1. Lithology, Sedimentology and Microfacies

The main lithology of Famennian and Dinantian carbonate sequences of the Central Carnic Alps comprises various types of bedded micritic Flaser-limestones covered by an irregular network of thin clayish seams. The biotic composition is dominated by cephalopods. With varying abundances also other pelagic groups occur such as trilobites, ostracodes, radiolarians and conodonts. Less abundant are echinoderms, molluscs, juvenile bivalves, brachiopods and fish teeth (see Plates 1, 2). Fossils are more abundant in the Kronhof Limestone, in particular, in bed nos. 3, 4 and 5. The Pal Limestone has only been studied in detail in its upper part. Conodonts, however, have also been recovered from the lower beds which are equivalent to the Upper expansa Zone.

This type of mainly goniatite bearing wackestone bridges the D/C boundary without any significant break. In terms of mapping units ("Formations"), the Famennian portion of the sequence constitutes the Pal Limestone while the equivalents of the Tournaisian represent the Kronhof Limestone. The latter are mainly light greyish to reddish and well bedded micritic limestones. The individual beds are separated by more or less distinct wavy bedding planes. Up to 1 cm thick clay partings are rather uncommon but occur between bed nos. 5a and 6d and between nos. 12 and 13.

The studied section comprises 15 limestone beds with varying thicknesses. At the boundary interval each thicker bed was further subdivided into smaller units to gain more detailed information about ranges of individual taxa. Thus during this study a total of 22 samples were collected and analyzed.

According to K. BOECKELMANN and L. KREUTZER who re-examined the petrographic data the upper part of Grüne Schneid section consists of the following lithologies (after H.P. SCHÖNLAUB et al., 1988, see Pl. 1, Figs. 1–8):

Bed 7/praesulcata Zone

18 cm thick greyish to slightly pink colored limestone bed with faint black veins; wackestone with tiny cephalopod shells, ostracodes, gastropods, trilobites, spheres (radiolarians ?) and crinoid stems.

Bed 6/praesulcata and sulcata Zone

32 cm thick light grey to yellowish and in part faintly pink colored limestone bed. Residual clay can either be arranged irregularly to form a network on the surface

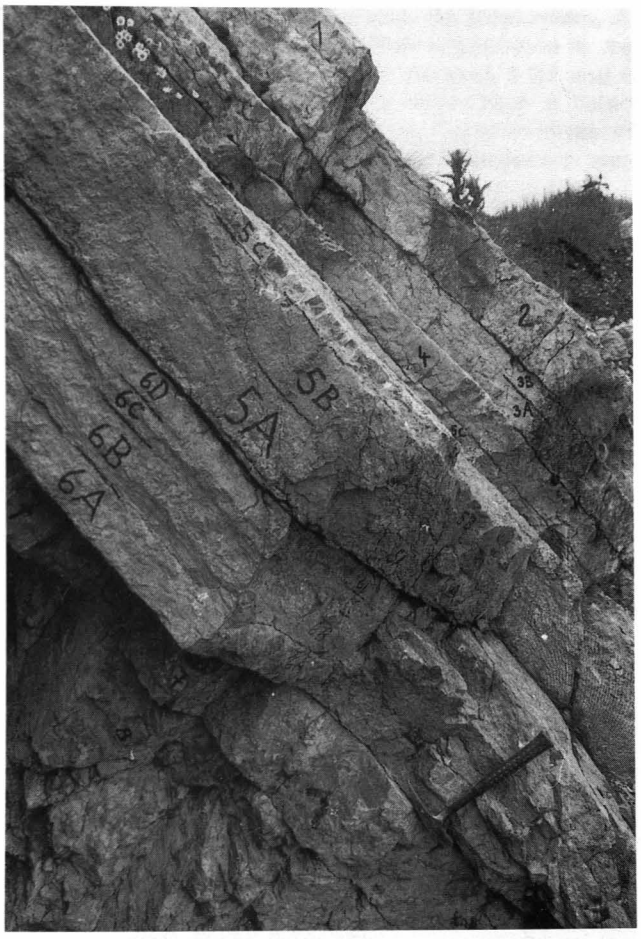

◀ b a ▲

Text-Fig. 3.
Grüne Schneid section.
A: Photograph shows the upper part of the section with bed nos. 8 to 1.
B: 32 cm thick bed no. 6 and its subdivision into 4 (5) subbeds numbered from base to top 6A, $6B_1$, $6B_2$, 6C, 6D.
D/C boundary between subbed nos. 6C and 6D. Note uniform lithology throughout the boundary bed.

or can be concentrated as clay parting parallel to bedding plane to indicate four indistinctly recognizable subbeds (6a–6d, see Text-Fig. 3 B). Subbed 6 B is divided into a 4 cm thick lower more argillaceous part (6 B1) and a 7 cm thick upper less clayish part (6 B2). The lower subbed 6 B1 comprises a bioclastic stylolitic and microstylolitic ostracode mudstone (micrite/siltite) with echinoderms and brachiopods. Subbed 6 B2 is a wackestone with small cephalopod shells and ostracodes, gastropods, trilobites, spheres, small bivalves and crinoid debris. Most shell debris is tiny and fragile. Inhomogeneous parts indicate bioturbation, clay enrichment point to locally strong solution processes.

Bed 5/sulcata to Lower duplicata (?) Zone

29 cm thick greyish to weakly pink colored limestone bed the lowermost 3 to 4 cm of which are distinctly pinkish colored. In this portion residual clay from pressure solution is more common than in the upper portion of the bed. The effect of solution can also be seen

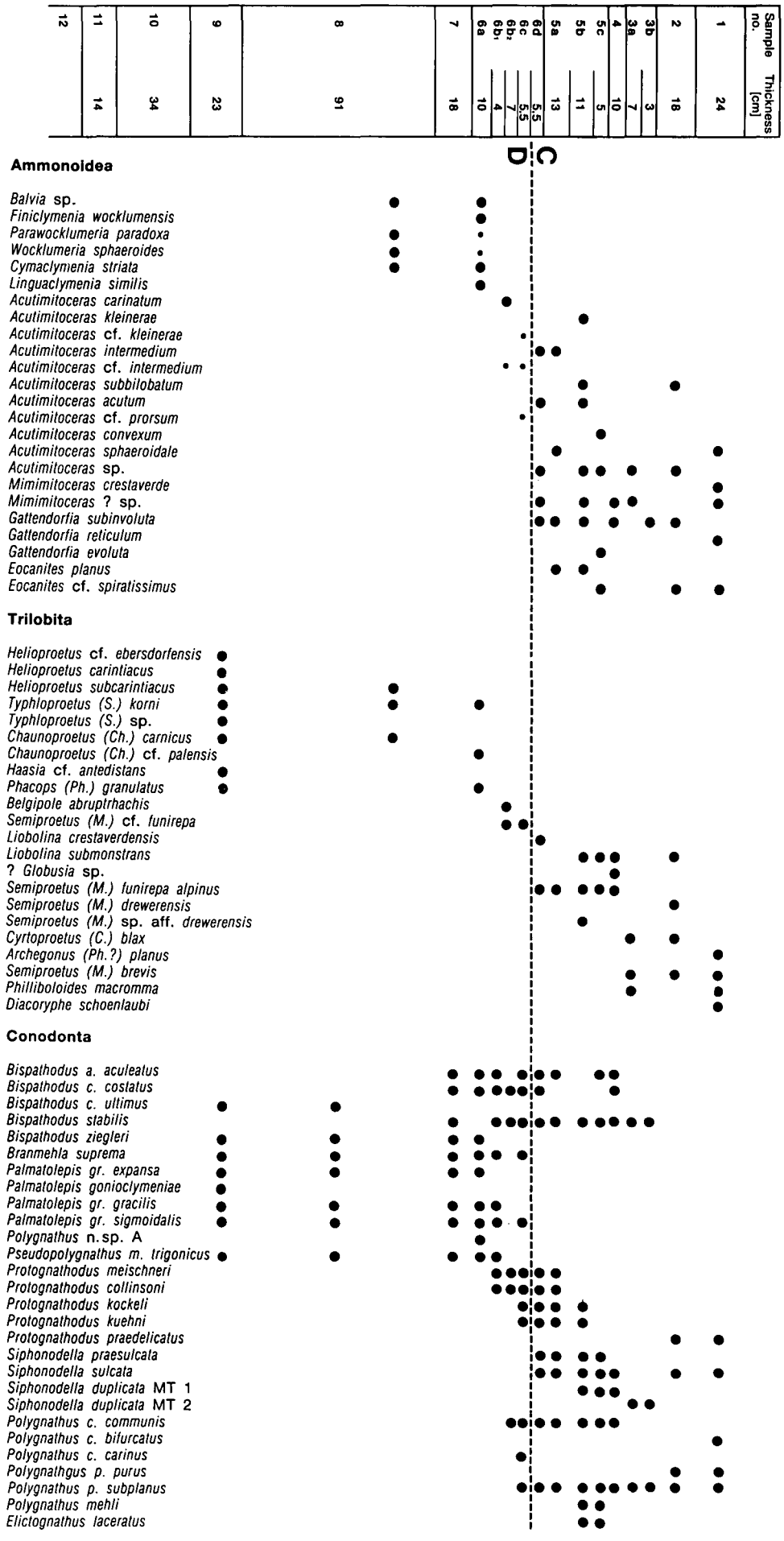

Text-Fig. 4.
Distribution of conodonts, ammonoids and trilobites at the Grüne Schneid section.

along the surface of individual cephalopod shells. Thin sections reveal a strongly bioturbated and mottled goniatite wackestone with some ostracodes, crinoid debris, spheres, few bivalves and trilobites. Geopetal fabrics are common in the whole bed.

Bed 4/duplicata Zone

10 cm thick light grey and well bedded limestone bed; goniatite wackestone with stylolitic fabric and large trilobite carapaces, ostracodes, bivalves and spheres.

Bed 3/duplicata Zone

10 cm thick light grey to yellowish/brownish and weakly pink colored limestone bed; bioturbated trilobite-goniatite-wackestone with few ostracodes, bivalves and crinoid debris, also showing stromatactis fabric with internal sediment.

Beds 2,1/duplicata Zone

18 and 24 cm thick limestone beds, respectively. Greyish micritic limestone beds, indistinctly pinkish colored. Thin sections reveal tiny goniatite shells as the main biotic constituent of the rock.

2.2. Paleontology

2.2.1. Conodonts

(H.P. SCHÖNLAUB)

The revised and updated conodont based subdivision of Grüne Schneid section is shown in Text-Fig. 4. The 4.95 m thick Upper Devonian sequence (sample nos. 15–6B) represents the Upper expansa and the Lower and Middle praesulcata Zones in the revised conodont zonation of W. ZIEGLER & C.A. SANDBERG (1984). A more precise assignment, however, is yet not possible due to the absence of the zonal index *Siphonodella praesulcata* on which this zonation has been based.

Sample 11 collected from 2.06–1.92 m below the D/C boundary contains, beside others, the last occurrences of such stratigraphically important species like *Palmatolepis gr. gonioclymeniae* together with *Bispathodus c. ultimus* and *B. ziegleri* suggesting the highest equivalents of the Lower praesulcata Zone.

The poorly defined Middle praesulcata Zone may be represented from sample 10 to sample 6 B, i.e., from 1.92–5.5 cm below the D/C boundary. In the following 5.5 cm thick subbed 6 C the entry of *Protognathodus kockeli* and *P. kuehni* were recognized. Its forerunners, *P. meischneri* and *P. collinsoni*, have their appearance in the bed below and were found in the samples 6 B1 and 6 B2. The accompanying conodont association is listed in Text-Fig. 4. Beside others a few representatives of *Palmatolepis (P. gr. sigmoidalis)* and *Branmehla suprema* survived into this level.

Subbed 6 D is characterized by the entry of the index conodont *Siphonodella sulcata*. It is associated with different species of *Bispathodus, Protognathodus, Polygnathus* and the first appearance of *Pseudopolygnathus dentilineatus*.

Additional and revised conodont data restrict the range of the sulcata Zone to the interval from samples 6 D to 5 C which corresponds to the basalmost 34.5 cm of the Lower Carboniferous. In the upper part of this bed *Siphonodella duplicata* Morphotype 1 appears. It is succeeded by a more advanced morphotype of *S. duplicata* in the samples 3 A and 3 B which we assign to *S. duplicata* Morphotype 2. The change of the conodont fauna from *S. sulcata* to *S. duplicata* Morphotype 1 is well recorded in our collection. It is in bed no. 5 and coincides with the last occurrences of representatives of the genus *Protognathodus*. As known from other sections *S. sulcata* co-occurs with *S. duplicata* in the upper part of the Grüne Schneid section.

In our conodont collection from beds just below and above the D/C boundary some juvenile platform elements of polygnathids with large basal cavity suggest a relationship with *Siphonodella sulcata*. As far as the lower surface is concerned also some representatives of the genus *Pseudopolygnathus* show a similarity with the zonal index. The main differences, however, are the flat platform and the weak development of a rostrum-like anterior trough, the more oval outline of the platform, the ornamentation of the platform with short but strongly developed transverse ridges and the more pronounced arching of the platform in lateral view. Until revision of the lowermost Carboniferous polygnathids we tentatively assign these specimens to *Polygnathus mehli* THOMPSON and perhaps *P. longiposticus* BRANSON & MEHL. Some of these platform conodonts are illustrated on Plate 3.

2.2.2. Ammonoids

(D. KORN)

The Devonian/Carboniferous boundary beds of the Grüne Schneid section yielded a rich collection of am-

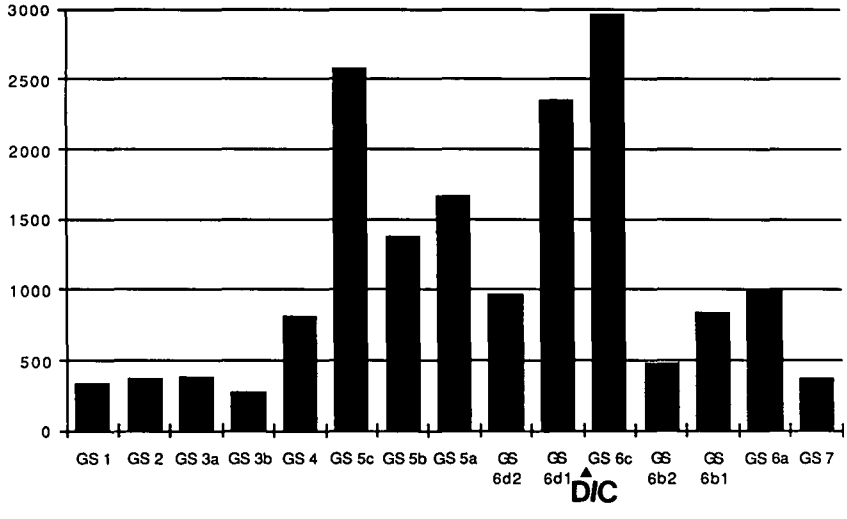

Text-Fig. 5.
Total counts of conodonts at the Grüne Schneid section, sample nos. 7 to 1.

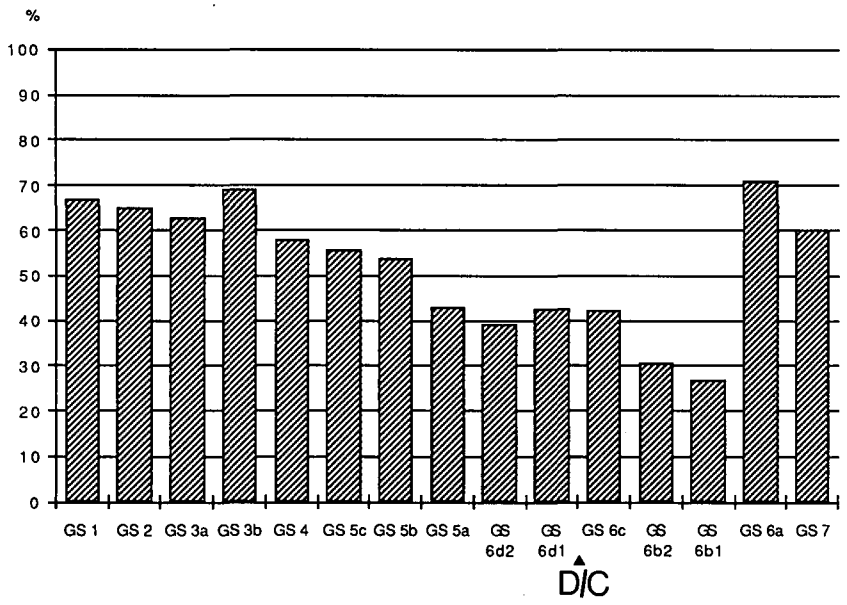

Text-Fig. 6.
Percentage of identified conodont taxa at Grüne Schneid, sample nos. 7 to 1.

monoids (D. KORN in H.P. SCHÖNLAUB et al., 1988; D. KORN, 1992, this volume). At hand are some 200 specimens which can be attributed to four different ammonoid horizons (see Text-Fig. 4). In successive order these are the Lower and Upper paradoxa Zones of the Wocklumeria Stage (Upper Devonian), the so-called *Acutimitoceras* fauna (prorsum Zone) of the uppermost Devonian, and the acutum Zone of the Gattendorfia Stage in the Lower Carboniferous.

Distribution and subdivision of the whole collection are shown in Text-Fig. 4 and illustrated on Plates 4 and 5:

Close to the base of bed no. 12 the occurrence of *Parawocklumeria paprothae* corresponds to the Lower paradoxa Zone.

In the uppermost 20 cm of bed no. 8 the following assemblage clearly indicates the Upper paradoxa Zone: *Wocklumeria sphaeroides, Parawocklumeria paradoxa, Cymaclymenia striata* (the only well preserved taxon), *Mimimitoceras* sp. and *Balvia* sp..

Bed no. 7 yielded only two indeterminable representatives of a clymeniid and a prionoceratid.

The following subbed no. 6 A contains the same fauna as in bed no. 8 supplemented by *Finiclymenia wocklumensis* and *Linguaclymenia similis*. This assemblage represents the Upper paradoxa Zone.

The 11 cm thick subbed no. 6 B can be subdivided into a lower 4 cm thick more argillaceous ammonoid-free horizon (6 B1) which presumably corresponds to the Hangenberg Shales of the Kronhofgraben section, and an 7 cm thick upper horizon (6 B2) characterized by small goniatites. In comparison with the underlying subbed no. 6 A the goniatite assemblage shows distinct differences. They belong to the genus *Acutimitoceras*; clymeniids have completely disappeared. In this association *Acutimitoceras carinatum* is well represented and thus indicates an equivalent level with the *Acutimitoceras* fauna of Stockum (D. KORN, 1984).

Subbed no. 6 C yielded similarly small representatives of the genus *Acutimitoceras*, i.e., *A.* cf. *prorsum and A.* cf. *kleinerae* corresponding to the prorsum Zone.

A major change occurs in the following subbed no. 6 D with the entry of *Gattendorfia subinvoluta* and *Acutimitoceras acutum*. This fauna clearly indicates the base of the Gattendorfia Stage of the Lower Carboniferous.

The succeeding sequence yielded a very similar goniatite fauna. At subbed no. 5 A the important index genus *Eocanites* appears. Based on this fauna the Carboniferous portion of the Grüne Schneid section can be assigned to the acutum Zone of the Gattendorfia Stage.

In summary, the Grüne Schneid section can easily be correlated with other D/C boundary sections, in particular with those from the northern margin of the Rhenish Massif (Oberrödinghausen, Müssenberg). However, none of these sections yielded a comparable complete succession of ammonoids across the D/C boundary beds.

2.2.3. Trilobites

(R. FEIST)

The new and amended list of trilobites from the Devonian/Carboniferous boundary section at Grüne Schneid is shown in Text-Fig. 4 and is illustrated on Plates 6–9 (R. FEIST, 1992, this volume).

Starting with bed no. 15 each layer yielded trilobites which belong to three successive associations. Based on more than 120 trilobite remains from bed no. 15 to the top of the section the following subdivision can be recognized (see Text-Fig. 4 and R. FEIST, 1992, this volume):

1) In the late Upper Devonian the *Helioproetus-Chaunoproetus* Association comprises both blind forms and those with reduced eyes.
2) The following abruptirhachis Association is characterized by normally oculated trilobites. This fauna is restricted to the subbeds 6 B2 and 6 C, i.e., the level following the "Hangenberg Event" and immediately below the D/C boundary.
3) A lowermost Carboniferous association consisting of *Liobolina* and *Macrobole* which exhibit only oculated forms although the size of the eyes is moderate.

The reduction of the eyes during the late Devonian Wocklumeria Stage presumably reflects an adaption to a deeper environment below the photic zone. The small size of all taxa, the reduction of prominent sculptural elements, the spinous character and the convex thorax suggest an endobenthic mode of life. This habit changed during the following time: the appearance of

trilobites with exclusively well developed eyes in subbed 6 B and the following horizon 6 C suggests a slightly shallower environment than before. The bathymetric change can be attributed to the final stage of the end-Devonian regression (O.-H. WALLISER, 1984; J.G. JOHNSON et al., 1985). This environment lasted through the following sulcata conodont zone although new forms appeared, but again changed at the beginning of the duplicata conodont zone when a slight deepening and thus a transgression is indicated by trilobites with reduced eyes which co-occurred with forms with normal eyes.

2.3. Conodont Biofacies

(R. DREESEN)

The conodont biofacies analysis of the Grüne Schneid section is based on countings from 15 samples and considers a total of almost 17.000 individual conodont elements with an average identification level of more than 50 % (Text-Figs. 5–7, R. DREESEN, 1992, this volume).

The older part of the *S. praesulcata* Zone is characterized by a palmatolepid-bispathodid (branmehlid) biofacies (Text-Fig. 7). The succeeding equivalents of the early Tournaisian Stage correspond to a polygnathid biofacies (average of over 85 %). Representatives of *Pseudopolygnathus* and of *Siphonodella*, however, do occur but their abundances are rather low when compared with the coeval Kronhofgraben section. An opposite relationship between the two sections is suggested by the representatives of the genus *Protognathodus* which occurs with significantly higher frequency in the Grüne Schneid section than at Kronhofgraben.

In the Grüne Schneid section the most dramatic change in conodont biofacies occurs below the *S. praesulcata/S. sulcata* zonal boundary, i.e., between subbeds nos. 6 A and 6 B (Text-Fig. 7). The sudden decrease of species of *Palmatolepis, Pseudopolygnathus* and *Branmehla* is contrasted by a striking increase of species of *Polygnathus* and of *Protognathodus*, suggesting a sudden lowering of sea-level as observed in many other sections around the world just before the D/C boundary. This level coincides with a change of the trilobite fauna, i.e., the change from trilobites with blind or reduced eyes to those with normal eyes (see Text-Fig. 4 and chapter on trilobites by R. FEIST, 1992, this volume).

3. Kronhofgraben Section

The Kronhofgraben section (Text-Fig. 2 B) is located some 9 km to the east of the Grüne Schneid section (H.P. SCHÖNLAUB, 1969a, 1985). In the tectonic framework of the Carnic Alps it belongs to a different unit, which originally was separated from the Grüne Schneid section more than 9 km to the northeast (H.P. SCHÖNLAUB, 1985).

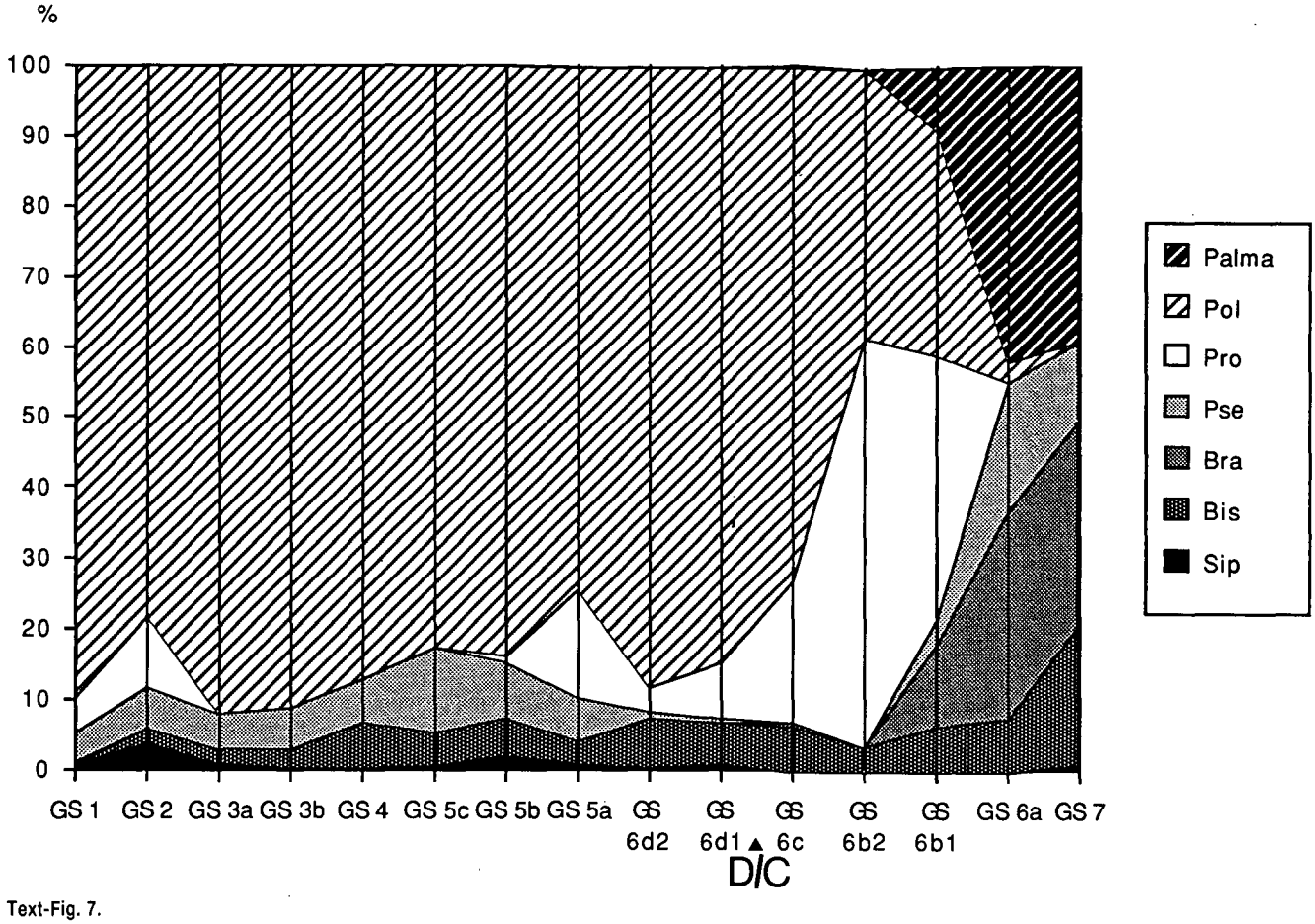

Text-Fig. 7.
Distribution [%] of important conodont genera across the D/C boundary at Grüne Schneid, sample nos. 7–1.
Abbreviations: D/C = Devonian/Carboniferous boundary; Palma = *Palmatolepis*; Pol = *Polygnathus*; Pro = *Protognathodus*; Pse = *Pseudopolygnathus*; Bra = *Branmehla*; Bis = *Bispathodus*; Sip = *Siphonodella*.

Text-Fig. 8.
Kronhofgraben section showing on the right, the uppermost part of the Devonian limestone sequence (Pal Limestone) followed by the black shale horizon and the Kronhof Limestone to the left.
At the left margin, the black bedded cherts form the top of the sequence.

The Kronhofgraben section is easily accessible through an alpine road running from Kronhof in the Gail valley via Untere to Obere Bischofalm (lower to upper Bischofalm). At an altitude of some 1360 m the road must be left to reach the section by a short footwalk along the small Aßnitz River (Text-Fig. 2B).

The excellently exposed D/C boundary beds crop out at an altitude of 1390 m on the eastern side of the upper Kronhofgraben (Text-Fig. 8). They belong to a folded Lower Devonian to Lower Carboniferous limestone sequence (H.P. SCHÖNLAUB, 1969b). The slightly overturned section comprises cephalopod limestones in the Famennian, followed by a 0.50 m thick shale horizon ("Hangenberg Black Shale") and a 81 cm thick limestone sequence named Kronhof Limestone. It is succeeded by some 4 m of black bedded radiolarian-bearing cherts with intercalations of three small limestone lenses (H.P. SCHÖNLAUB, 1969a; G. HAHN & R. KRATZ, 1992, this volume).

In the following chapters additional data are presented which update and revise an earlier publication on the Kronhofgraben section by the first author in 1969.

3.1. Lithology, Sedimentology and Microfacies

The lithology of the Upper Devonian to Lower Carboniferous Kronhofgraben section comprises different rock types (Pl. 2, Figs. 1–10). The Devonian portion consists of the Pal Limestone while the Carboniferous part is attributed to the Kronhof Limestone (Text-Fig. 8).

The Upper Devonian limestone sequence is composed of indistinctly bedded greyish bioclastic mud/wackestones with ostracodes, echinoderms and some cephalopods. Very abruptly this limestone succession is followed by a 50 cm thick unfossiliferous black shale horizon rich in pyrite. Due to compression its lateral equivalent may be reduced to a thickness of less than 25 cm. Tests for spores by M. STREEL (Liège) were thus far negative.

The overlying 81 cm thick grey Kronhof Limestone comprises 6 limestone beds of varying thicknesses. The basalmost bed no. K12 is 15 cm thick; it is followed by bed no. K13 with a thickness of 13 cm. The next 28 cm thick bed is subdivided into a lower 4 cm thick subbed no. K14 and an upper 24 cm thick subbed no. K15 which is overlain by the 18 cm thick bed no. K16. This bed is succeeded by the 6 cm thick bed no. K17 and the 1 cm thin bed no. K18. Sample K19 was collected from a limestone lense intercalated in the cherts some 80 cm above the topmost limestone bed.

According to K. BOECKELMANN the Kronhofgraben section comprises the following lithologies (Pl. 10, Figs. 1–10):

Bed no. K1/praesulcata Zone

The uppermost 3 cm thick portion of the Pal Limestone is a bioclastic Mud-/wackestone (homogeneous micrite) with echinoderms, ostracodes, fragments of trilobites, a few shell debris of molluscs and fragments of cephalopods. Small areas are dolomitized and numerous thin calcite veins intersect the rock vertically.

Bed no. K12/sulcata Zone

The 15 cm thick bed consists of a microstylolitic ostracode mudstone with low fossil content (some shell debris). The sediment is rich in insoluble residue and has partly altered into an unfossiliferous microsparite and fine-grained sparite. Thick calcitic fissures are abundant.

Bed no. K13/sulcata Zone

13 cm thick limestone bed composed of bioclastic mud-/wackestone (homogeneous micrite) with brachiopods, molluscs, ostracodes, a few echinoderms, trilobites, radiolarians and goniatites. Numerous thin and broad fissures.

Subbed no. K14/duplicata Zone

This 4 cm thick subbed shows the same lithology as the bed below.

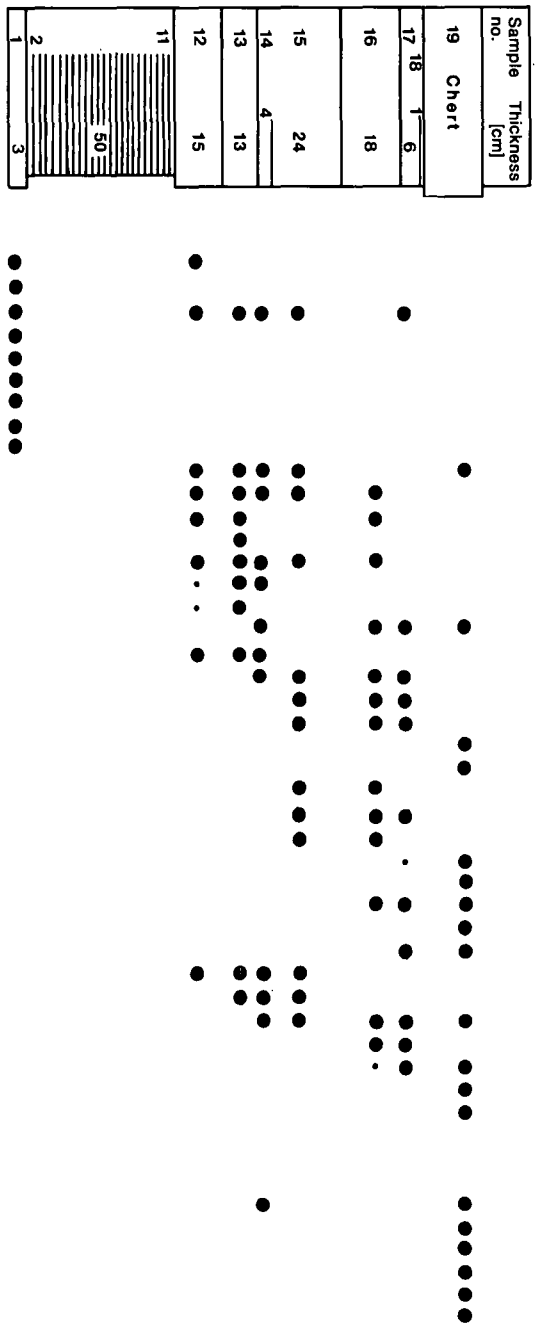

Text-Fig. 9.
Distribution of conodonts and trilobites in the Kronhofgraben section, sample nos. K1 to K19.

Subbed no. K15/duplicata Zone

24 cm thick ostracode mudstone (micrite/siltite) with some trilobites, radiolarians and shell remains. Thick calcite fissures intersect this bed.

Bed no. K16/duplicata Zone

18 cm thick limestone bed displaying a mudstone (homogeneous micrite) with echinoderms, molluscs, ostracodes, cephalopods and radiolarians. Horizontally orientated fenestral fabrics occur in one layer. Broad calcitic veins are abundant.

Bed no. K17/duplicata Zone

The 6 cm thick bed comprises relicts of a mudstone (homogeneous micrite) with shell remains of ostracodes and molluscs. Most of the original sediment is altered into an inhomogeneous fine- to medium-grained unfossiliferous sparite intersected by many veins.

Bed no. K18/duplicata Zone

The topmost 1 cm thick bed of the Kronhof Limestone comprises a bioclastic mudstone (homogeneous micrite) with bioclasts of brachiopods and molluscs.

Limestone lense no. K19/sandbergi Zone

10–15 cm grey limestone lense; bioclastic wackestone and packstone (micrite and fine-grained sparite) with fragments of conodonts, trilobites, ostracodes, echinoderms and molluscs. A broad fissure seems to be filled with a fault breccia composed of coarse-grained calcite and fragments of micrite sediment.

*

The main differences between the Grüne Schneid and Kronhofgraben sections concern the dominating cephalopod limestones at Grüne Schneid which indicate bioturbation, and generally contain more fossils par-

ticularly of goniatites and echinoderms. The lithology of the Kronhofgraben section is dominated by non-bioturbated ostracode mudstones with only few bioclastic components of echinoderms and brachiopods.

3.2. Paleontology

3.2.1. Conodonts

(H.P. SCHÖNLAUB)

The revised and updated conodont association and its distribution at the Kronhofgraben section is shown in Text-Fig. 9. Following the conodont zonation proposed by W. ZIEGLER & C.A. SANDBERG (1984) the Famennian to Lower Tournaisian sequence represents the Upper praesulcata, sulcata, duplicata and the basal part of the sandbergi Zones.

The uppermost 3 cm thick bed of the Pal Limestone (K1) yielded a conodont fauna diagnostic for the Upper praesulcata Zone. From the succeeding 50 cm thick pyritiferous shales neither any conodonts nor any other fossils, e.g., spores were yet recovered.

Sample K12 from the base of the Kronhof Limestone contains the name bearer of the sulcata Zone, *Siphonodella sulcata*, together with representatives of the *Protognathodus* fauna. This co-occurrence suggests that the Upper praesulcata Zone defined by the appearance of *Protognathodus kockeli* below the entry of *S. sulcata* may be partly represented by the equivalent of the Hangenberg Black Shale. The base of bed no. K12 may thus be correlated with bed no. 6 D or an even higher level at the Grüne Schneid section.

The next although not well defined change of the conodont fauna occurs at the base of bed no. K13 or subbed no. K14 with the appearance of morphotypes of *Siphonodella duplicata*. Evidently, at the latter horizon *S. duplicata* Morphotype 2 is present. This horizon correlates with bed nos. 5 or 4 of the Grüne Schneid section.

The following conodont fauna from samples K16 to K19 has not been recorded at Grüne Schneid section. The most plausible explanation is the extended range of Kronhofgraben section in comparison with the short Grüne Schneid section. This concerns representatives of the genus *Siphonodella*, e.g., *S. carinthiaca, S. cooperi, S. lobata* and *S. sandbergi*. The latter two are restricted to the limestone lense no. K19 within the chert horizon.

3.2.2. Ammonoids, Trilobites

(G. HAHN, R. KRATZ)

A relatively brief test on ammonoids resulted in only few badly preserved and undeterminable cephalopods. Trilobites, too, were only recovered from two levels, i.e., subbed no. K14 (*Diacoryphe* sp.) and the limestone lense no. K19 within the chert horizon (Text-Fig. 9). According to G. HAHN & R. KRATZ (1992, this volume) the assemblage consists of some 60 trilobite remains. They belong to exclusively blind representatives of the genera *Diacoryphe* (50 %), *Silesiops (Chlupacula)* (25 %) and *Liobolina* (25 %). In addition some fragments of *?Silesiops* and *?Archegonus (Phillibole)* were found.

The trilobite assemblage recovered from the Kronhofgraben section represents a deep water community which has not been known from any other area of the Culm basin yet. Different from well known trilobites of the Culm shales with reduced eyes this fauna suggests a completely dark environment. It may be best characterized as the impoverished "Hangenberg Fauna" of the Grüne Schneid section which in its upper part contains trilobites with blind and reduced eyes (R. FEIST, 1992, this volume).

3.3. Conodont Biofacies

(R. DREESEN)

The following conodont biofacies analysis is based on countings from 8 samples resulting in a total of more than 14.000 conodont elements with some 60 % of identified taxa (Text-Figs. 10–12).

Similar to the Grüne Schneid section, the praesulcata Zone is represented by a palmatolepid-bispathodid (branmehlid) biofacies, followed during the early Tournaisian sulcata and duplicata Zones by a polygnathid biofacies. Due to the intercalation of shales this change in biofacies is indicated in our file very abruptly (Text-Fig. 12). In comparison with the Grüne Schneid section, data from Kronhofgraben show a higher frequency of representatives of *Pseudopolygnathus* and a striking increase of "pelagic" species of *Siphonodella* (Text-Fig. 12) suggesting a sudden deepening for the Kronhofgraben depositional area during the *S. sandbergi* Zone. This conclusion is in perfect accordance with thin section data as well as with biological considerations inferred from trilobites. The most striking difference between the Grüne Schneid and Kronhofgraben sections during the sulcata Zone is the occurrence of a

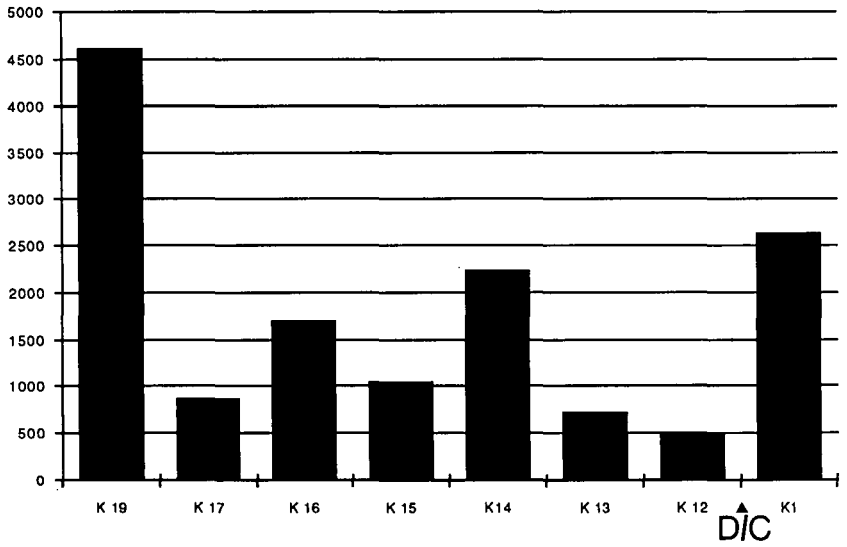

Text-Fig. 10.
Total counts of conodonts in the Kronhofgraben section, sample nos. K1 to K19.

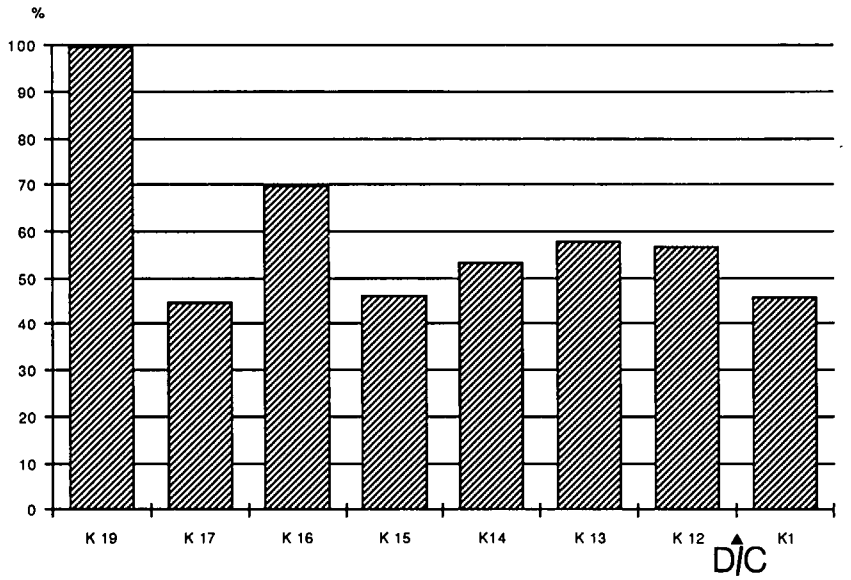

Text-Fig. 11.
Percentage of identified conodont taxa in the Kronhofgraben, sample nos. K1 to K19.

distinct *Protognathodus* population (almost 30 %) at Grüne Schneid (Text-Fig. 7). The contrasting relationship in Kronhofgraben may result from the fact that during that particular time interval shales were deposited.

4. Mineralogy, Geochemistry and Stable Isotopes of the Grüne Schneid and Kronhofgraben Sections

4.1. Mineralogy

(A. FENNINGER)

Based on XRD (Cu, K alpha, 30 KV, 20 MA, 1°/min) of randomly orientated total sample analysis the Upper Devonian Pal Limestone and the Lower Carboniferous Kronhof Limestone of the Grüne Schneid section consist of mainly calcite with minor contents of quartz and dolomite. A similar composition is also suggested for the Devonian/Carboniferous rocks at Kronhofgraben section although the contents of quartz and pyrite varies to a certain extent (Text-Fig. 13). In this section the dolomite content may increase to a value of 6.45 % as analyzed for sample K12. In the shaly interval the illite/muscovite content increases considerably to match the amount of quartz. The accompanying fairly high content of FeS_2, calculated between 6 and 11 % by P. KLEIN and C. ORTH (Text-Fig. 14), suggests a pyritifer-

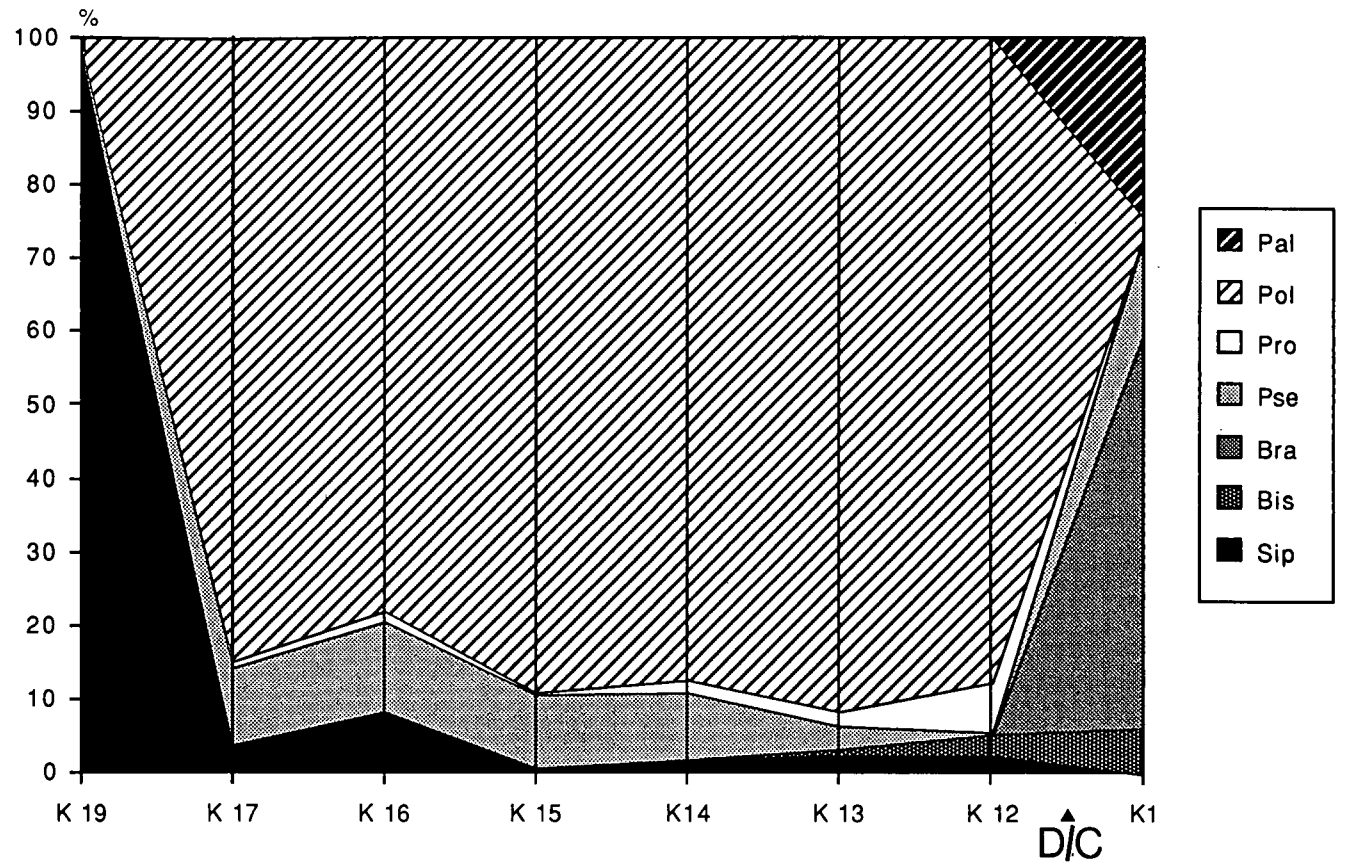

Text-Fig. 12.
Distribution [%] of important conodont genera in the uppermost Devonian and Tournaisian of the Kronhofgraben section, sample nos. K1 to K19.
For abbreviations see Text-Fig. 7.

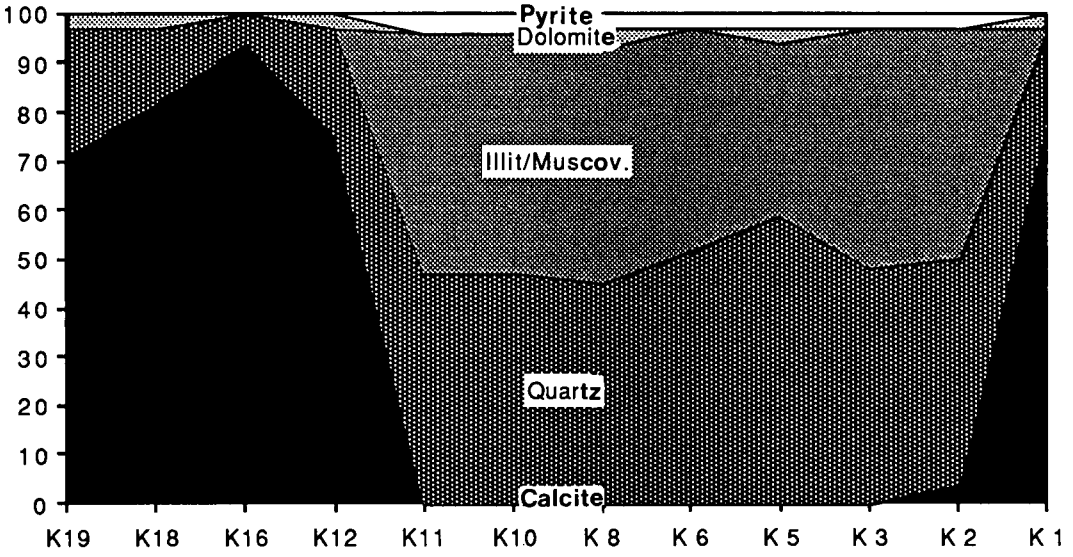

Text-Fig. 13.
Mineralogy of the Kronhofgraben section inferred from XRD data.
Sample no. K1 from top of the Upper Devonian Pal Limestone, sample K2 to K11 from the 50 cm thick pyritiferous shale horizon equivalent to the Hangenberg Black Shale, and sample nos. K12 to K18 from the Kronhof Limestone. Sample K19 from the limestone lense within the black cherts (sandbergi Zone).
D/C boundary is between K10 and K11.

ous shale composed of predominantly illite/muscovite, quartz and iron sulfide.

Of primary interest was the determination of total sulfur, S_{tot}, which represents S as pyritic sulfur. According to X-ray diffraction analysis (A. FENNINGER) pyrite was expected to be the main component of the shale unit at Kronhofgraben section. In fact, most of the sulfur was insoluble in HCl. Acid-soluble sulfur was found in only minor proportions. The high content of organic carbon particularly in the lower part of these shales is of further interest (Table 2). Obviously it is related to the high S content and the locally high contents of heavy metals like Cr, Co, Cu, Ni and Pb (see Tables 2 and 3).

The results obtained from XRD agree well with those calculated from the analytical determinations (see Text-Figs. 14 and 15).

In all samples of the Grüne Schneid section the $CaCO_3$ content varies between 92.6 and 99.4 %; quartz is an additional but only minor constituent. According to XRD-data the content of $CaCO_3$ may be as low as 92.9 % for subbed 5 A and 92.6 % for the oldest Carboniferous limestone bed no. 6 D. The relatively low content of $CaCO_3$ in subbed 6 B confirms the biostratigraphically derived conclusions that it may correspond with the shale horizon of the Kronhofgraben section.

4.2. Common and Trace Elements I (ICP, AAS, LECO)

(P. KLEIN)

Common and trace elements were analyzed through inductively coupled plasma-atomic spectrometry (ICP) and atomic absorption spectrometry (AAS). Carbon and sulfur were determined through combustion analysis and infrared detection. The individual methods applied to samples from the two sections are thoroughly described by P. KLEIN (1991).

The analytical results obtained from the D/C boundary beds in the Grüne Schneid section suggest an overall uniformity for the section below and above the

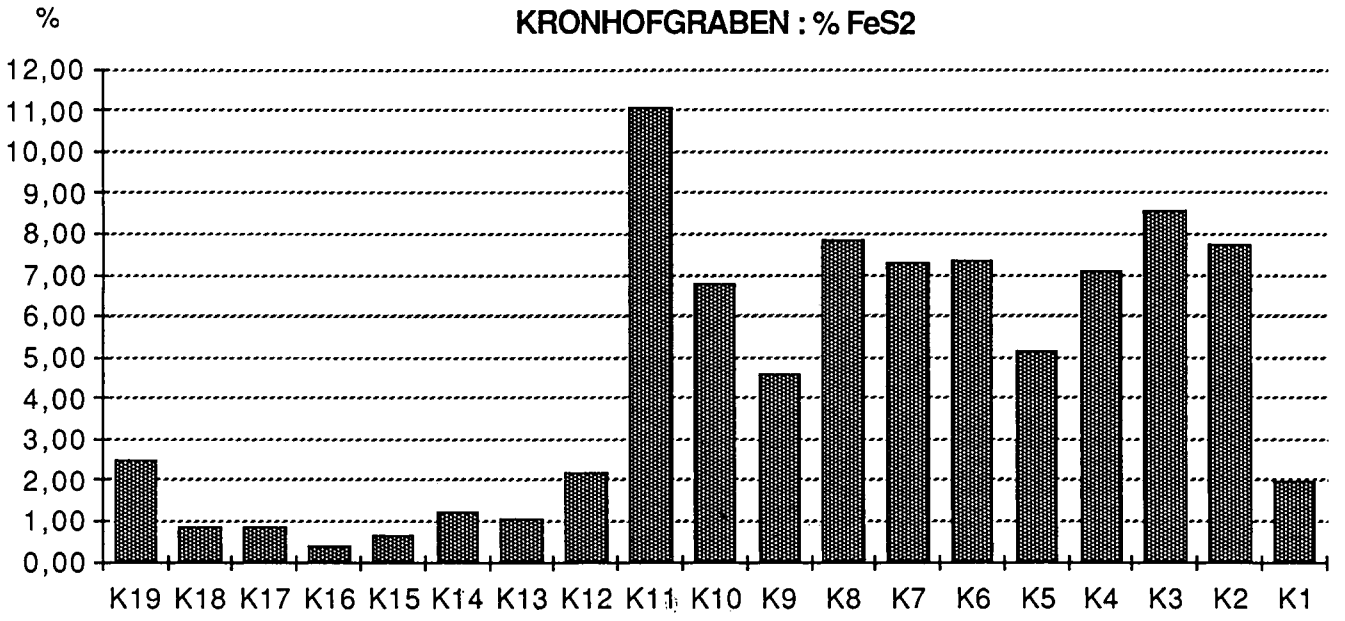

Text-Fig. 14.
Plot of FeS_2 content [%] in samples from the Kronhofgraben according to values of Table 1.
For this tabulation the lower contents of Table 1 were used as Fe may also be represented in other mineralogical compositions.

Table 1.
Content of FeS_2 in samples K1 to K19 of the Kronhofgraben section.
A) Conversion of ORTH's Fe values into % pyrite (conversion factor 2.148280).
B) Conversion of KLEIN's S values into % pyrite (conversion factor 1.870868).
The variation between the two data sets of ORTH and KLEIN originates from calculating the sulfur or the iron values for the amount of FeS_2. Bold numbers are considered to represent the "true" amounts as Fe may also be represented in other compositions.

Sample nr.	A (INAA) [% FeS_2]	B (ICP, AAS) [% FeS_2]
K 1	2.2	**2.00**
K 2	10.1	**7.76**
K 3	**8.6**	9.52
K 4	**7.1**	9.06
K 5	**5.2**	5.84
K 6	10.5	**7.36**
K 7	7.9	**7.32**
K 8	**7.9**	8.05
K 9	6.5	**4.59**
K10	7.9	**6.83**
K11	11.4	11.10
K12	2.7	**2.21**
K13	1.6	**1.09**
K14	1.8	**1.23**
K15	1.2	**0.67**
K16	0.5	**0.42**
K17	**0.9**	0.97
K18	1.1	**0.90**
K19	**2.5**	2.90

boundary. The only exceptions are significantly higher Ba and moderately changed Mn contents for limestones below and above the D/C boundary. Considerably higher contents of Co, Cu, Ni and Zn, however, occur in a thin shale parting between sample nos. 6 D and 5 A (Text-Fig. 16).

The analytical results from the Kronhofgraben section display a similar pattern as those from the Grüne Schneid section (Table 2). However, in the 50 cm thick shale horizon, there is a distinct signal from heavy metals, more especially high contents of Co, Cr, Cu, Ni, Pb. Moreover, high contents have been recorded also of organic carbon, sulfur, arsenic, antimony, uranium, and lanthanum, as well as of dysprosium and ytterbium (as representatives of rare earth elements), see Table 3.

4.3. Common and Trace Elements II (INAA, RNAA)

(C.J. ORTH, M. ATTREP)

Instrumental neutron activation analysis (INAA) provided by the Los Alamos Research Reactor Group were applied to all samples from the Grüne Schneid and Kronhofgraben sections to determine the whole-rock abundances for common and trace elements. Radiochemical methods were performed to measure the Ir content of some selected samples from the boundary zone (Text-Figs. 17,18,19, Table 3). For details of the laboratory techniques the reader is referred to M. ATTREP et al. (1991).

Comments

On Text-Fig. 18 we show 16 plots to illustrate certain points for the D/C interval measurements. Yet at this boundary there is no evidence in the crucial elemental data to indicate a large-body impact. If one did occur it will be necessary to demonstrate it from physical signatures such as microspherules or shocked mineral grains.

1) Although at Kronhofgraben section Ir shows some enhancement from normal crustal values (between 55 ppt to 140 ppt) in the 50 cm thick shale horizon, so do most other elements.
2) The Ir taken as a ratio to Al (Al is representative of the clay fraction; thus Ir is normalized to clay content) shows a dip in the shale as compared with the carbonates below and above.
3) The Ir/Cr pattern can provide some information about possible extraterrestrial contributions to the

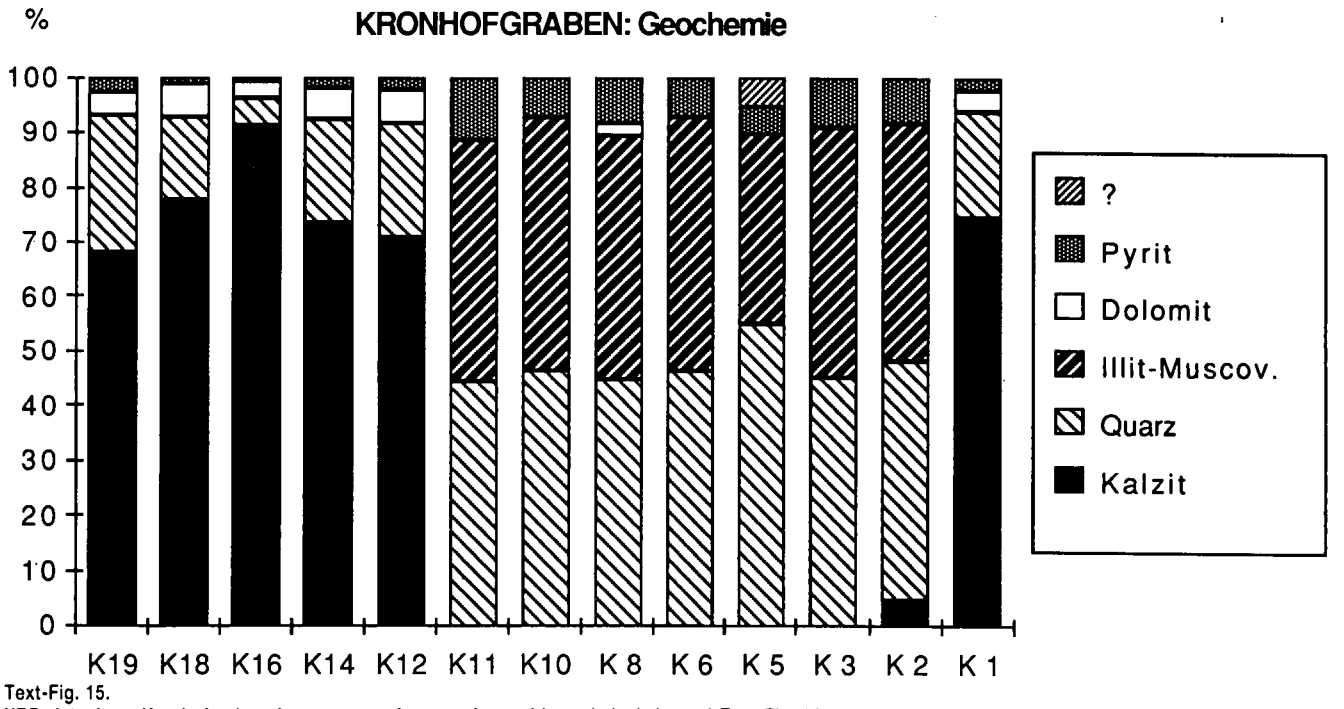

Text-Fig. 15.
XRD-data from Kronhofgraben for purpose of comparison with analytical data of Text-Fig. 14.

Table 2.
Geochemistry of common and trace elements using ICP, AAS and LECO for the D/C boundary beds in the Kronhofgraben.

																				HCl-soluble carbonate fraction [%]									
Nr.	Res.	Al	Ba	Ca	Co	Cr	Cu	Fe	K	Mg	Mn	Na	Ni	P	Pb	Sr	Ti	V	Zn	C_{tot}		C_{org}		C_{carb}	S_{tot}		S_{org}		$S_{HCl-sol}$
	[%]	[%]	[ppm]	[%]	[ppm]	[ppm]	[ppm]	[%]	[ppm]	[%]	[ppm]	[ppm]	[ppm]	[ppm]	[ppm]	[ppm]	[ppm]	[ppm]	[ppm]	x	s	x	s		x	s	x	s	
K 1	19.1	0.02	55	32.0	1	1	1	0.18	195	0.55	750	195	4	340	6	305	4	1	11	9.64	0.024	0.194	0.014	98	1.07	0.01	1.02	0.02	4.7
K 2	98.0	0.05	55	0.25	3	2	18	0.50	455	<0.01	20	500	6	360	60	2	3	2	4	11.93	0.030	11.63	0.030	2.5	4.15	0.05	3.85	0.09	7.2
K 3	98.5	0.04	29	0.08	2	2	16	0.25	335	<0.01	23	156	10	160	45	< 1	2	1	3	12.55	0.010	12.37	0.120	1.4	5.09	0.04	4.60	0.15	9.6
K 4	98.4	0.04	23	0.07	1	2	14	0.31	355	<0.01	18	120	3	130	35	< 1	2	1	3	11.54	0.070	11.24	0.050	2.6	4.84	0.03	4.32	0.03	10.7
K 5	98.5	0.04	26	0.04	1	2	7	0.29	320	<0.01	19	115	2	90	20	< 1	2	< 1	3	10.47	0.190	10.19	0.040	2.7	3.12	0.06	2.70	0.01	13.5
K 6	97.0	0.04	42	0.17	2	2	2	0.40	315	<0.01	13	108	2	25	15	1	1	1	4	4.33	0.070	4.23	0.070	1.0	3.93	0.07	3.40	0.15	13.5
K 7	98.8	0.04	20	0.05	6	2	12	0.16	325	<0.01	44	114	11	45	21	< 1	2	1	3	0.905	0.011	0.890	0.001	1.6	3.91	0.12	3.32	0.01	15.1
K 8	95.0	0.07	40	1.05	13	2	3	0.34	560	0.33	760	122	24	1000	13	8	4	1	4	1.106	0.004	0.660	0.020	40	4.30	0.04	3.66	0.01	14.9
K 9	97.9	0.04	85	0.18	3	2	6	0.34	365	<0.01	49	114	3	160	45	1	2	1	4	9.09	0.045	8.844	0.110	2.8	2.45	0.01	2.21	0.05	9.8
K10	98.4	0.06	46	0.30	16	2	15	0.20	535	0.02	148	116	12	150	40	3	3	1	7	0.699	0.001	0.615	0.012	12	3.65	0.04	3.20	0.14	12.3
K11	97.9	0.08	51	0.30	9	<1	16	0.31	630	0.01	70	123	16	980	31	5	3	1	3	0.897	0.023	0.873	0.005	2.7	5.93	0.04	4.58	0.07	22.8
K12	22.3	0.02	85	30.5	2	<1	< 1	0.28	170	0.85	730	186	6	125	5	255	3	1	9	9.13	0.060	0.079	0.001	99	1.18	0.01	1.17	0.01	< 1
K13	13.2	0.02	85	34.0	< 1	<1	< 1	0.21	182	0.80	730	165	2	155	3	265	2	1	5	10.20	0.030	0.057	0.002	99	0.581	0.003	0.572	0.001	1.5
K14	12.4	0.01	140	35.0	< 1	<1	< 1	0.21	161	0.75	728	180	2	195	4	305	2	2	10	10.39	0.090	0.100	0.005	99	0.658	0.003	0.646	0.003	1.9
K15	7.7	0.01	150	37.5	< 1	<1	< 1	0.15	90	0.60	732	180	1	240	3	300	2	1	6	10.60	0.160	0.092	0.001	99	0.356	0.002	0.350	0.001	< 1
K16	5.6	0.01	40	38.5	< 1	<1	< 1	0.07	71	0.37	550	150	2	230	4	250	1	1	9	10.87	0.010	0.075	0.014	99	0.224	0.006	0.220	0.006	< 1
K17	8.4	0.01	50	37.0	< 1	<1	5	0.06	75	0.60	515	150	2	105	1	250	2	1	7	10.72	0.010	0.080	0.002	99	0.515	0.020	0.512	0.009	< 1
K18	15.0	0.01	50	34.0	< 1	<1	12	0.13	125	0.80	750	170	3	105	6	275	2	1	10	9.93	0.032	0.081	0.003	99	0.482	0.016	0.480	0.015	< 1
K19	25.9	0.02	40	29.0	< 1	<1	1	0.11	132	0.55	800	185	6	870	9	240	3	10	6	8.94	0.015	0.220	0.002	98	1.55	0.02	1.45	0.01	6.5

Sample no.	Thickness [cm]	Res. [%]	Al [%]	Ba [ppm]	Ca [%]	Co [ppm]	Cu [ppm]	Fe [%]	K [ppm]	Mg [%]	Mn [ppm]	Na [ppm]	Ni [ppm]	P [ppm]	Pb [ppm]	Sr [ppm]	Zn [ppm]	C_{tot} [%] x	s	C_{org} [%] x	s	C_{carb} [%]	S_{tot} [ppm] x	s	S_{org} [ppm] x	s
1	24																									
2	18	3.1	0.02	10	40.50	< 1	4	0.08	295	0.04	500	114	2	130	1	281	8	11.40	0.10	0.075	0.004	99	170	8	105	7
3b	3	4.9	0.01	6	39.00	1	1	0.09	145	0.21	650	83	3	96	7	220	6	11.10	0.06	0.074	0.001	99	165	9	100	5
3a	7																									
4	10	4.0	0.01	5	39.50	7	2	0.08	189	0.21	700	87	3	102	2	230	7	11.20	0.12	0.170	0.015	98	150	10	75	10
5c	5	4.6	0.01	6	39.10	2	4	0.16	304	0.24	1600	125	2	125	10	320	10	11.27	0.02	0.130	0.015	99	138	4	80	4
5b	11	4.4	0.01	9	39.00	2	5	0.22	220	0.24	870	106	2	140	10	290	8	11.05	0.05	0.080	0.008	99	125	2	63	6
5a	13	8.6	0.02	14	37.20	5	9	0.29	276	0.20	2300	102	6	182	15	270	7	10.50	0.13	0.065	0.003	99	135	9	75	10
D/C ▶ 6d	5.5	32.0	0.05	48	27.40	10	12	0.24	167	0.23	700	77	21	695	6	140	16	10.83	0.06	0.062	0.009	99	1550	50	1500	30
◀ 6c	5.5	9.5	0.01	11	37.10	3	11	0.56	372	0.25	2050	213	6	103	12	220	6									
$6b_2$	7	6.8	<0.01	46	37.80	5	3	0.19	200	0.21	1900	94	4	115	11	252	11	10.90	0.15	0.077	0.007	99	172	8	130	5
$6b_1$	4																									
6a	10	3.2	0.01	44	40.10	5	4	0.14	224	0.23	1330	102	4	148	11	282	12	11.25	0.09	0.111	0.011	99	125	9	75	9
7	18	3.3	<0.01	25	39.80	2	2	0.17	184	0.17	950	94	2	280	6	245	6	11.15	0.02	0.080	0.003	99	145	5	64	10
8	91																									
9	23																									
10	34																									
11	14																									
12																										

Text-Fig. 16.
Geochemistry of common and trace elements using ICP, AAS and LECO for the D/C boundary beds at Grüne Schneid.

Table 3.
Abundances of 20 common, trace, rare earth and Pt-group elements obtained by INAA and RNAA for the D/C boundary beds in the Kronhofgraben.

Sample	Instr. no.	x_1 x_2 [cm]	Na [ppm]	Mg [%]	Al [%]	Ca [%]	Sc*) [ppm]	V [ppm]	Cr*) [ppm]	Mn [ppm]	Fe*) [%]	Co*) [ppm]	As [ppm]	Sb [ppm]	La [ppm]	Ce	Yb [ppm]	Hf	Ir [ppT]	Th*) [ppm]	U [ppm]	C_{org} [%]	Sm [ppm]	Dy [ppm]
19	1001	0 20	4900	0.75	1.35	32.0	4.4	122	19	1090	1.16	8	23	2.8	20.7		2.07		65	2	4.03	0.221	4.0	3.7
18	1002	20 21	3010	0.80	1.17	34.4	2.4	10	6	1160	0.52	6	4.5	0.66	18.5		1.56		32	2	0.84	0.081	4.7	3.6
17	1003	21 29	1950	0.65	0.63	39	1.5	7	9	810	0.41	2	2.7	0.43	9.1		0.82			2	0.57	0.080	1.9	1.8
16	1004	29 49	530	0.40	0.39	36.8	1.1	8	4	720	0.28	4	3.3	0.62	7.1		0.5		23	1	0.38	0.075	1.1	1.1
15	1005	49 70	1150	0.63	0.78	38.0	2.1	10	9	1010	0.57	8	5.9	0.54	11.9		0.86			2	0.57	0.092	2.0	1.7
14	1006	70 76	800	0.64	1.06	35.5	3.0	17	12	1320	0.86	4	6.5	0.66	16.4		1.10		48	3	0.69	0.100	2.6	1.5
13	1007	76 89	710	0.88	1.30	37.7	2.8	12	10	1350	0.73	8	7.5	0.75	13.4		1.03			3	0.64	0.057	2.2	1.5
12	1008	89 106	800	0.80	1.01	29.0	3.0	19	5	1640	1.26	12	9.4	1.7	15.6		1.83		42	3	1.36	0.079	4.2	3.3
11	1009	106 111	2300	0.90	10.2	0.35	20.7	206	96	640	5.31	58	47	7.2	115		8.9			23	11.9	0.873	18.9	15.5
10	1010	111 116	2600	0.72	9.80	0.22	18.4	144	89	468	3.7	73	50	7.2	81		5.7		122	19	10.4	0.615	10.7	7.7
9	1011	116 121	1250	0.56	7.60	0.1	15.3	351	86	202	3.04	17	52	16	90		8.0			17	24.0	8.84	12.5	15.0
8	1012	121 126	1340	0.96	8.90	0.7	16.7	141	84	1210	3.7	41	23	3.1	102		7.7		71	18	10.0	0.66	18.6	16.3
7	1013	126 131	1790	1.10	11.1	0.1	20.3	194	118	376	3.7	64	62	9.3	94		6.3			22	12.6	0.89	11.5	8.1
6	1014	131 136	800	0.72	7.90	0.1	13.7	284	83	55	4.9	15	80	21	69		4.9		55	14	12.4	4.23	10.7	9.3
5	1015	136 141	1520	0.55	7.20	0.1	14.8	297	71	142	2.97	8	39	15	87		8.1		54	15	23.2	10.2	13.0	12.3
4	1016	141 146	2700	0.58	7.20	0.1	14.6	331	77	192	3.32	13	33	15	88		7.1		82	15	25.3	11.2	12.6	13.2
3	1017	146 151	2350	0.67	7.40	0.1	18.9	386	91	264	4.0	20	57	18	99		9.5		98	19	28.0	12.4	15.3	13.5
2	1018	151 156	1580	0.56	7.40	0.2	20.4	478	125	174	4.7	21	62	19	111		10.3		140	19	28.6	11.6	18.5	17.3
1	1019	156 160	680	0.64	1.14	34.8	3.9	19	15	970	1.04	10	19	1.7	19.5		2.5		67	3	2.73	0.19	4.4	3.8

*) Preliminary result.

weak Ir anomaly in the shales. The solar system ratio of Ir/Cr is about 4.9×10^{-5}. The background Ir/Cr level from our plot is between 4 to 6×10^{-6} in the limestones and is less than 2×10^{-6} in the shales. This ratio is typical of terrestrial rocks and more than an order of magnitude smaller than chondritic. The Ir/Cr and Ir/Sc patterns are relatively flat, indicating all three elements were about equally incorporated in the sediments.

4) The moderate Ir anomaly in the shale appears to have resulted from incorporation in a combination of the shale and the high content of the organic carbon (up to 12.37 %, see Table 2) which resulted in reducing conditions. This behaviour has been observed at other similar horizons in the geologic record too (C.J. ORTH, 1989; C.J. ORTH et al., 1986, 1988; M.W. WALLACE et al., 1990, 1991). Microorganisms, e.g., certain bacteria are mainly hold re-

Sample no.	Thickness [cm]	U [ppm]	Th [ppm]	Ba [ppm]	As [ppm]	Mn [ppm]	V [ppm]	Ti [ppm]	Ca [%]	K [ppm]	Al [ppm]	Mg [ppm]	Na [ppm]
1	24												
2	18	0.11	0.83	<200	4.5	420	< 6	<4000	37	1300	3200	3100	119
3b	3												
3a	7	0.16	1.42	<300	8.9	660	10	<5000	40	2600	5600	3100	138
4	10	0.13	1.05	<200	14.6	630	<10	<6000	42	1800	4500	<3000	136
5c	5	0.15	1.25	<200	2.7	1350	13	<8000	41	2300	5100	3000	140
5b	11	0.11	1.18	<130	7.9	720	8.7	<3000	37	1950	5000	2800	130
5a	13	0.17	1.57	<300	5.9	1650	<11	< 0.7	39	3000	0.64	3200	145
▶ 6d	5.5	0.29	2.51	<170	21	1900	28	< 0.6	37	4700	1.02	2400	216
6c	5.5												
$6b_2$	7	0.29	1.73	88	17.1	1470	14	< 0.4	36	2800	0.66	2700	157
$6b_1$	4												
6a	10	0.16	1.01	<200	12.2	1020	< 7	<. 0.5	41	1600	0.33	<1800	105
7	18	0.16	0.48	<180	9.1	840	<10	<6000	44	1300	3400	<3000	99

◀

Text-Fig. 17.
Abundances of 12 common and trace elements obtained by INAA for the D/C boundary beds at Grüne Schneid.

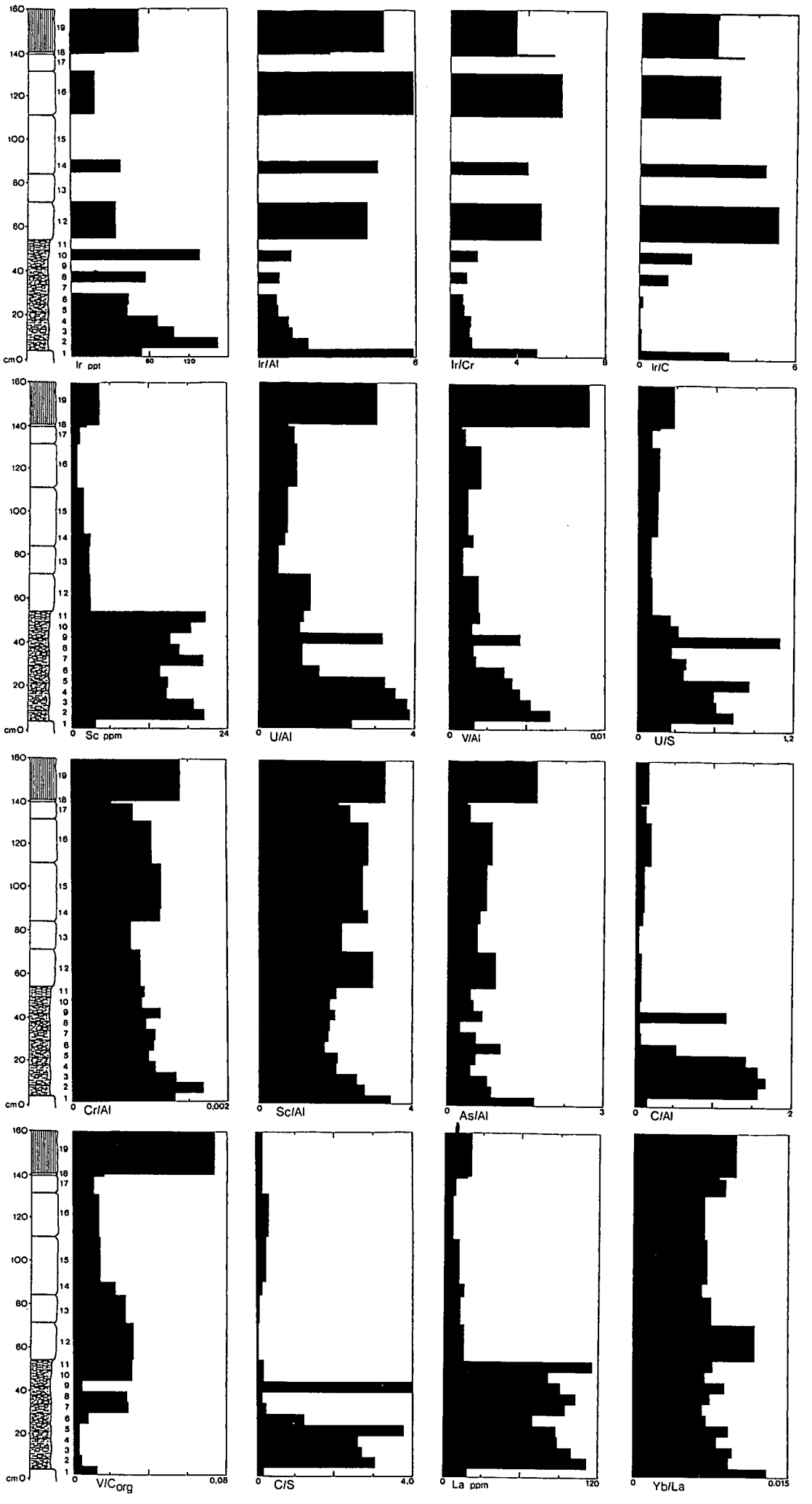

Text-Fig. 18.
Plots for selected elements and elemental ratios from the D/C boundary beds of the Kronhofgraben section.

sponsible for the Ir enrichments as they are capable to extract it from seawater (B.D. DYER et al., 1989).

5) The U and V data suggest that these two elements also are probably hosted by a combination of the clay and the organic carbon in the shale, and not by the organic sulfur. $C_{(org)}$ and $S_{(org)}$ data of Table 2 are used to make further comparisons.
6) The Cr/Al, Sc/Al and As/Al patterns are relative flat. They were plotted to check for possible excess chromite and if sedimentation perhaps derived from source rocks of more mafic or ultramafic composition in the shale. Apparently there is little (sample No. K2) or no indication for this assumption.
7) Some rare earth distributions were plotted and the patterns show a slight Ce anomaly for carbonates as might be expected from deposition from sea water. The shale samples are representative of rare earth ratios of continental sediments. Mafic to ultramafic rocks show some enhancement of these heavy rare earths, which these samples do not.
8) The Grüne Schneid data shown on Text-Figs. 17 and 19 generally have a similar behaviour to those of the Kronhofgraben section. The Ir signal displays normal crustal values.

In summary, the D/C anomalies (enrichments), if they can be seen at all, appear to be the result of oceanic geochemical processes, but it is difficult to provide a solid explanation merely from these data.

4.4. Carbon and Oxygen Isotopes

(M. MAGARITZ)

The distribution of the stable isotopes of carbon and oxygen may provide information about seawater salinity and temperature and variations in the carbon cycle between the inorganic and organic reservoirs. Decrease in productivity (mass extinction) or increase in the rate of oxidation of buried organic matter, for example as a result of regression, will shift the surface ocean marine bicarbonate reservoir toward negative ^{13}C values while increase in productivity and organic matter

Sample no.	Thickness [cm]	Ir/Al × 10^{-9}	Ir [ppb]	Carbon Isotopes $\delta^{13}C$	Oxygen Isotopes $\delta^{18}O$
1	24				
2	18			2.33	-9.5
3b	3			2.25	-9.1
3a	7				
4	10			2.29	-9.1
5c	5			2.40	-9.4
5b	11	5.4	0.027	2.52	-9.1
5a	13	4.6	0.043	2.64	-8.9
		4.2	0.027	2.70	-9.0
▶ 6d	5.5	4.3	0.044	2.58	-9.3
6c	5.5				
6b₂	7				
6b₁	4	2.9	0.019	2.96	-9.3
6a	10	7.0	0.023	2.53	-8.9
7	18			2.31	-9.6

Text-Fig. 19.
Ir content, Ir/Al ratio and isotope geochemistry of the D/C boundary beds in the Grüne Schneid section.

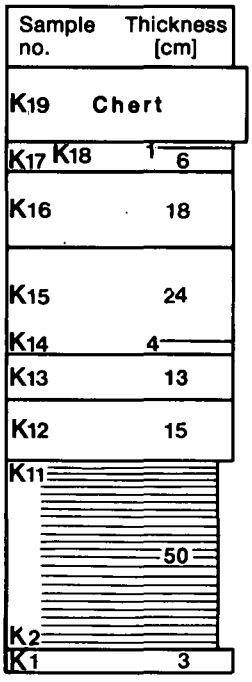

$\delta^{18}O$	$\delta^{13}C$
-7.8±0.14	-0.26±0.10
-8.0±0.15	0.13±0.06
-7.3	1.38
-7.6	1.67
-7.1±0.15	1.53±0.07
-7.7	1.40
-7.5	1.62
-7.2±0.08	1.96±0.06
-5.9	1.19
-8.0	-0.36
-6.4±0.07	1.43±0.05
-7.6	1.54

Text-Fig. 20.
Oxygen and carbon isotope ratios of the D/C boundary beds in the Kronhofgraben section.

burial will shift the reservoir toward ^{13}C enrichment. Most of the studied era or period boundaries associated with mass extinction events exhibit large changes in the carbon cycles, which are characterized first by a carbon isotope shift toward negative $\delta^{13}C$ values and then by a positive shift (M. MAGARITZ, 1989, 1991).

During the Carboniferous, the carbon isotopes of marine carbonate are enriched in ^{13}C relative to present day oceans, but show sharp negative excursions at stage boundaries (M. MAGARITZ & W.T. HOLSER, 1990).

The data from the D/C boundary interval of Grüne Schneid and Kronhofgraben are provided in Text-Figs. 19 and 20. At both localities there is no change in the carbon isotope composition across the boundary which may reflect a major mass extinction or any other unusual turnover. Note that the Kronhofgraben section is depleted by about 1‰ in $\delta^{13}C$ relative to the Grüne Schneid section (i.e., they are slightly enriched in the light isotope ^{12}C) which may relate to a diagenetic calcite associated with the high organic matter content found in this sequence. Another explanation for the carbon isotope change is the distinctly different environments of deposition: The shallow sea (Grüne Schneid section) where bicarbonate ions are enriched in ^{13}C due to high productivity as opposed to the deeper sea (Kronhofgraben) where dissolved bicarbonate ions were relatively depleted in ^{13}C. Some change in the carbon isotope composition seems to occur between sample nos. K17, K18 and K19, respectively. This level coincides with the transition from the limestone dominated sequence to black radiolarian cherts characterized by blind deep-water trilobites and a peculiar conodont association (see biostratigraphic chapters in this report). Whether or not this drop in $\delta^{13}C$ is a local signature is yet unclear, but the change in facies may not rule it out.

The low $\delta^{13}C$ values of the shale samples nos. K9 und K10 should be considered with reservation due to

the very low carbonate content which may include some secondary calcite formed by oxidation of organic derived carbonate ions. Note that these rock samples are characterized by high contents of organic carbon.

During the late Paleozoic the $^{18}O : ^{16}O$ ratio in seawater (= $\delta^{18}O$) was rather constant and ranged between −1 and 0 ‰ (T.F. ANDERSON, 1990). Records from marine cements of Carboniferous age indicate slightly lower values (B.N. POPP et al., 1986; J. VEIZER et al., 1986).

The oxygen isotope records from Grüne Schneid and Kronhofgraben sections show no distinct changes across the D/C boundary (Text-Figs. 19,20). However, the Grüne Schneid section displays slightly lower values of about 2 ‰ in $\delta^{18}O$ relative to the Kronhofgraben section. These variations may be related to different water salinities or temperatures in the two settings or may be related to a relatively higher degree of oxygen isotope alteration during diagenesis. The fact that the thermal histories of the two sections (see section 5) are similar, and that the sections represent shallow and deep sea environments respectively, may support the former hypothesis.

5. Thermal Overprint

(J.-M. SCHRAMM)

The Devonian/Carboniferous boundary beds of the Grüne Schneid section are part of the highest tectonic unit within the structural framework of the Central Carnic Alps. However, the Kronhofgraben section situated some 9 kilometers to the east, belongs to a deeper tectonic setting than the Grüne Schneid section. This whole area was affected by Variscan and Alpine tectonism and metamorphism. Consequently, a varying intensity of burial overprint can be expected depending on the primary position of the two localities during the Variscan and Alpine orogenetic events.

Apparently, metamorphic alterations of fossils in both sections are of minor significance. A low grade of burial metamorphism is documented by the conodont color alteration index (CAI) which varies for the Grüne Schneid section between 3.5 and 4.5 and which reaches 5 at Kronhofgraben. Preservation of ammonoids and trilobites is relatively good although collecting of fossils in the hard rock is a very strenuous matter. Nevertheless faint details of the eyes of trilobites are excellently preserved as are the ornamentation and the suture lines of ammonoids.

According to J.-M. SCHRAMM 1991 a more objective information on the degree of metamorphism of both sections is provided by the study of the illite crystallinity. This method is based on the determination of illite polytypes and selected lattice constants of illite or muscovite (see e.g., M. FREY (ed.), 1987, and others). For preparation of the samples, the actual determination of the illite crystallinity (IC) and the limiting values of the temperature-crystallinity correlations expressed in the "KUBLER-Index" we refer to J.-M. SCHRAMM (1991).

Text-Fig. 21 summarizes the IC data from the Kronhofgraben and Grüne Schneid sections (J.-M. SCHRAMM, 1991, Text-Fig. 3). In the first section the anchimetamorphic overprint affects the whole sequence. All available IC data suggest a temperature influence of approximately 300° which accords well with the CAI values.

The Grüne Schneid section reflects anchimetamorphic conditions in its lower part and diagenetic overprints in the uppermost bed nos. 1 and 2. This very low-grade metamorphism caused only moderate equilibrations of the ordering of the sheet-silicate. For this effect a temperature of 200° or less may be estimated.

6. Summary and Conclusions

Our multidisciplinary study on the Devonian/Carboniferous boundary of the Central Carnic Alps provides a well founded data base to reconstruct the

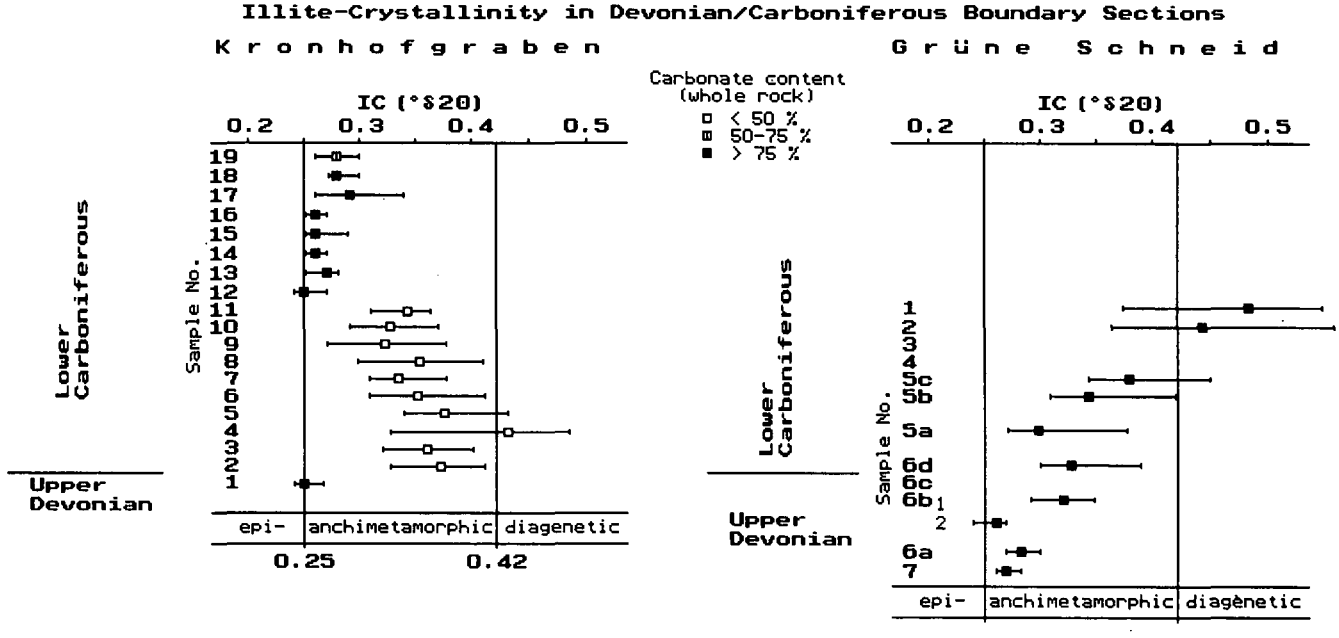

Text-Fig. 21.
Vertical trends of illite crystallinity (IC) in the D/C boundary beds of the Kronhofgraben and Grüne Schneid sections (modified from J.-M. SCHRAMM, 1991). Note that sample nos. 2 to 11 of Kronhofgraben represent the shale horizon; revised D/C boundary at Grüne Schneid between sample nos. 6C and 6D.

paleoenvironment of this specific area some 353 Ma ago. Lines of evidence include lithological, paleontological, mineralogical, geochemical and isotopic data from the uppermost Devonian Pal Limestone, the D/C boundary horizon, the equivalent of the Hangenberg Black Shale and the lowermost Carboniferous Kronhof Limestone. Our data are derived from the Grüne Schneid and Kronhofgraben sections which represent two distinct paleosettings. The two sequences are correlated by means of conodonts, ammonoids and trilobites. They occur in great abundances and variety across the boundary interval.

The D/C boundary as defined by the Working Group and ratified by ICS of IUGS in 1990, has been precisely recognized in our studied sections. At Grüne Schneid it is placed within the 32 cm thick limestone bed no. 6 and more precisely, between subbed nos. 6 C and 6 D. At Kronhofgraben the D/C boundary corresponds to the base of bed no. K12. At both localities it coincides with major faunistic changes. A significant biotic crisis, however, can not be recognized at this level.

We feel that the Grüne Schneid section is best suited as stratotype for the D/C boundary. It fulfils all physical, sedimentary and biological requirements which are needed to serve as an international reference section for the transition from the Devonian to the Carboniferous Period. Presently, however, we are not able to recognize the evolutionary sequence between *Siphonodella praesulcata* and *S. sulcata*.

The 6 m thick D/C boundary beds of the Grüne Schneid section are excellently exposed and display a uniform lithology, dominated by well bedded greyish cephalopod limestones. The conformable sequence is rich in macro- and microfossils, in particular conodonts, ammonoids and trilobites. According to the petrographic analysis based on thin sections, the lithology comprises bioturbated wackestones with ostracodes, echinoderms, trilobites, goniatites, brachiopods, spheres (radiolarians ?) and bivalves. There is no evidence of a break in the sequence nor of any major change of the paleoenvironment.

Study of the Grüne Schneid section started 4.95 m below the D/C boundary in the late Devonian Pal Limestone, which correspond to the Upper expansa through Lower and Middle praesulcata conodont zones. In the upper part of bed no. 6 they are succeeded by the equivalents of the Upper praesulcata Zone (sample no. 6C). This horizon represents a thickness of 5.5 cm. The following subbed no. 6D yielded the lowermost representative of *Siphonodella sulcata*, the index conodont for the base of the Carboniferous. The final 91 cm thick sequence represents the sulcata and parts of the following duplicata Zones.

The distinct subdivision of the section based on conodonts is equally duplicated by ammonoids and trilobites. In successive order the Lower and Upper paradoxa Zones of the Wocklumeria Stage were recognized (bed nos. 12 to 6A) followed by the equivalents of the *Acutimitoceras* fauna of Stockum in subbed nos. 6B and 6C. In the next subbed 6D a major change occurs showing the entry of index goniatites of the Gattendorfia Stage.

Trilobites belong to three successive associations which start in the late Upper Devonian with blind forms or those with reduced eyes (*Helioproetus-Chaunoproetus* association). The following abruptirhachis association is restricted to subbed nos. $6B_2$ and 6C. This fauna is characterized by normally oculated trilobites suggesting a slightly shallower environment than in the beds below. Such favourable conditions existed through the following sulcata Zone. During this lapse of time trilobites were characterized by normal eyes. At the onset of the duplicata Zone, however, deepening is indicated by the appearance of trilobites with reduced eyes.

Obviously, the successive changes of the fauna were related to moderate changes of sea level. This suggestion seems well constrained by the conodont biofacies analysis which indicates an open marine palmatolepid-bispathodid biofacies for the late Upper Devonian followed by a polygnathid biofacies during the Tournaisian. The most dramatic change occurs between subbed nos. 6A and 6B showing a sudden decrease of species of *Palmatolepis, Pseudopolygnathus* and *Branmehla* which is contrasted by a striking increase of species of *Protognathodus* and *Polygnathus*. Interestingly this level coincides with a change in the trilobite fauna.

The available geochemical data on common and trace elements as well as on stable isotopes of carbon and oxygen confirm the conclusions drawn above. Neither is there any change of isotopes across the D/C boundary indicating perhaps cessation of primary production in the surface ocean or significant temperature changes nor is there any other significant elemental variation except for the Ba and the Mn contents at either side of the boundary. Concentrations of Co, Cu, Ni and Zn, however, do occur in a 5 mm thick clay parting between sample nos. 6D and 5A immediately above the D/C boundary bed no. 6.

In summary, the Grüne Schneid section suggests an overall stable and moderately deep open marine environment across the D/C boundary. Subtle changes of sea level, however, did occur and can be recognized in the variation of the fauna, in particular in depth related changes of the trilobites and in the composition of conodonts. Such an event can be recognized at the base of subbed no. $6B_1$. At this level a lowering of sea level is suggested which, however, was of moderate extent and did not affect the sedimentation pattern. Retreat of the sea occurred shortly before the D/C boundary and lasted through the sulcata Zone but may have changed at the beginning of the following duplicata Zone when a deeper environment was established.

Comparison between the Grüne Schneid and the coeval Kronhofgraben sections reveals significant differences. The latter represents a deep-water off-shore limestone sequence with intercalation of a 50 cm thick shale horizon, known elsewhere as "Hangenberg Black Shale". In fact, as far as lithology and age are concerned this rock from the Carnic Alps closely resembles the Hangenberg Black Shale from the Rhenish Mountains. According to F. EBNER (1973) it is distributed also in other parts of the Carnic Alps.

Examination of the lithofacies, analysis of the conodont biofacies and distribution and composition of the macrofauna indicates for the sequence at Kronhofgraben a deeper environment than for the Grüne Schneid section. For example, if any, in the Lower Carboniferous Kronhof Limestone only blind trilobites occur; in comparison with Grüne Schneid the conodont biofacies is characterized by a striking increase of representatives of the "pelagic" genus *Siphonodella* and

decreased abundances of species of *Protognathodus*; and the lithofacies shows mainly non-bioturbated ostracode mudstones with only few bioclastic components.

The 50 cm thick pyritiferous shale intercalation between the Pal and the Kronhof Lsts. is correlative with subbed no. $6B_1$ of Grüne Schneid section which shows a slightly increased clay content. Based on goniatites, trilobites and conodonts the age of this horizon corresponds to the *Acutimitoceras* fauna of Stockum and hence belongs to the prorsum goniatite Zone of the uppermost Devonian. In terms of the presently used conodont zonation it belongs to the Middle and perhaps also to the Upper praesulcata Zones.

ICP, INAA and RNAA profiles across the limestone-shale sequence and in particular in the latter indicate that the shale horizon is moderately to strongly enriched in various sidero, chalco and lithophile elements relative to the surrounding limestone and to the limestones at the Grüne Schneid section, like Ir, Ni, Cr, Fe, Co, Pb, Cu, As, Sb, S and also of organic carbon, Sc, U, Th, V and La, Dy and Yb of selected rare earth elements. The highest Ir concentration ranges from 55 to 140 ppt suggesting a mean twofold enhancement as compared with the background level in the limestones. Locally the FeS_2 content increases to more than 11 %.

Yet we have not examined the boundary beds for the presence of any shock-induced lamellar deformation features or any other impact related physical evidences. The signatures presented above, however, lead us to conclude that these elemental enrichments were caused by oceanic geochemical processes and not by a large body impact.

Although there are no evidences at the Kronhofgraben section of negative excursions of the marine $\delta^{13}C$ or dramatic changes of the oxygen isotopes which very often are associated with Period and Stage boundaries, mass extinction and establishment of a "Strangelove ocean" (K.J. HSÜ & J.A. MCKENZIE, 1985; L.R. KUMP, 1991), the 50 cm thick shale intercalation suggests a significant "event" of starvation that affected the sedimentary environment at the closure of the Devonian. Supposedly, this event is related to the same changes of sea-level as concluded for the Grüne Schneid section. If so these shales must be regarded as "regressive black shales". However, we rather consider them as submerged deep water deposits formed below the maximum carbonate production in an aphotic stagnant basin under reducing conditions. Such a setting is consistent with our lithological, geochemical and paleontological results presented in the forgoing chapters. In this model strong subsidence was rather caused by tectonism prior to the Variscan orogenetic climaxes than by rapid rise of sea-level and a regional transgression of the shoreline. This explanation does not contradict with the conclusions reached for the Grüne Schneid section suggesting moderate regressive events involved at this locality at the end of the Devonian.

7. Plea for Reconsideration of Grüne Schneid Section as Global Stratotype for the D/C Boundary

During the meeting of the Devonian/Carboniferous Boundary Working Group at Courtmacsherry, Ireland (May 22–28th, 1988) four sections were discussed and considered as the final stratotype, i.e. La Serre (France), Hasselbach (Germany), Nanbiancun (China) and Grüne Schneid (Austria). However, the latter seems the only one that fulfils all criteria which are required as a worldwide stratotype summarized by the Guidelines of ICS of IUGS (J.W. COWIE et al., 1986).

La Serre, France

Although recently this section has been very well studied and documented (see G. FLAJS et al. [Eds.], 1988) and the transition from *Siphonodella praesulcata* to *S. sulcata* is well known some 90 % (!) of the fauna (and of the rocks) of the critical boundary interval are reworked in an oolitic sequence (R. DREESEN, unpubl. note, 1988). Hence, at this level many uncertainties may exist, beside the fact that the D/C boundary sediments were not deposited in an open marine environment. From the sedimentological as well as geological and biostratigraphical point of view the final choice of La Serre section as international stratotype for the D/C boundary was of great disadvantage.

Hasselbachtal

As early as 1984 it became clear that *S. sulcata* in bed no. 84 was reworked in a turbidite layer. Although rich in miospores and also goniatites (with some restrictions) this sequence lacks the required conodont data, i.e., the *S. praesulcata–S. sulcata* transition which defines the boundary. An additional disadvantage is the fact that the suggested boundary is close to the Hangenberg Shale/Hangenberg Limestone change and not within a uniform and continuous lithology.

Nanbiancun

This fossiliferous section (C.M. YU [Ed.], 1988) represents an extremely shallow neritic and not an open marine environment. Cephalopods are rare and yet poorly studied; conodonts, however, are fairly abundant. As far as the boundary is concerned there are disagreements among conodont workers in the taxonomic treatment of *S. sulcata* and its ancestor *S. praesulcata*.

Grüne Schneid

As shown above and in the accompanying papers of this volume the sequence at Grüne Schneid exhibits most requirements for the international stratotype for the D/C boundary:

- Continuous lithology of cephalopod limestones (wackestones) across the D/C boundary;
- Occurrence of *S. sulcata* (but not in a phyletic relationship as required by the Working Group on the D/C boundary);
- The boundary sequence does not show any shaly intercalations, nor any breaks or indications of reworking of rocks or faunas;
- Abundances of fossils, e.g., ammonoids, trilobites and conodonts in great numbers, and gastropods, bivalves, ostracodes, echinoderms and radiolarians as additional faunal constituents;
- Successive appearances of different associations of ammonoids, trilobites and conodonts of high correlative value as shown in this volume;
- Study of geochemistry, lithofacies and stable isotopes confirms the assumption of a uniform litholo-

gy in an open marine and stable subsiding environment,
and

- finally the Hangenberg Event was only of minor significance.

To conclude the excellent and well preserved outcrop contains tons of rocks which are easily accessible and can be richly collected for different fossil groups. This updated and revised version of the locality Grüne Schneid may further help to reconsider the decision on the global stratotype for the D/C boundary already made in 1990.

Plate 1

Microfacies of the D/C boundary beds at the Grüne Schneid section (after K. BOECKELMANN in H.P. SCHÖNLAUB et al., 1988, modified).

Fig. 1: **Wackestone (biomicrite) with cephalopd shells, ostracodes and spheres (radiolarians ?).**
Sample 7, Middle praesulcata Zone, late Famennian.
Scale: 3 mm.

Fig. 2: **Wackestone (biomicrite) with cephalopod shells, ostracodes and bivalves.**
Sample 6A, Middle praesulcata Zone, late Famennian.
Scale: 3 mm.

Fig. 3: **Radiolarian (?) wackestone (biomicrite) with strong influence of pressure solution.**
Sample 6B, Upper praesulcata Zone, late Famennian.
Scale 5: mm.

Fig. 4: **Wackestone (biomicrite) with ostracodes, bivalves and a large gastropod.**
Sample 6D, sulcata Zone, early Tournaisian.
Scale: 5 mm.

Fig. 5: **Stylolitic radiolarian wackestone (biomicrite) rich in insoluble residue.**
Note shelter porosity below the bivalve.
Sample 5 A, sulcata Zone, early Tournaisian.
Scale: 6.5 mm.

Fig. 6: **Goniatite wackestone (biomicrite) with some ostracodes.**
Sample 5 B, Lower duplicata Zone, early Tournaisian.
Scale: 6mm.

Fig. 7: **Cephalopod-radiolarian (?) wackestone (biomicrite) with orthoconic cephalopods (orthoceratids) and trilobites.**
Sample 5 C, Lower duplicata Zone, early Tournaisian.
Scale: 3.5 mm.

Fig. 8: **Radiolarian (?) wackestone (biomicrite) with ostracodes and a large trilobite.**
Note shelter porosity below the trilobite. A fenestral fabric (right) is filled at the base with internal sediment and on top with coarse-grained cement.
Sample 3, duplicata Zone, early Tournaisian.
Scale: 4 mm.

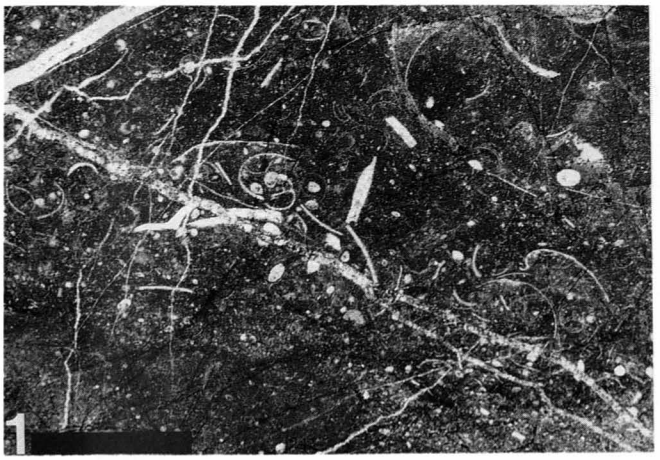
1

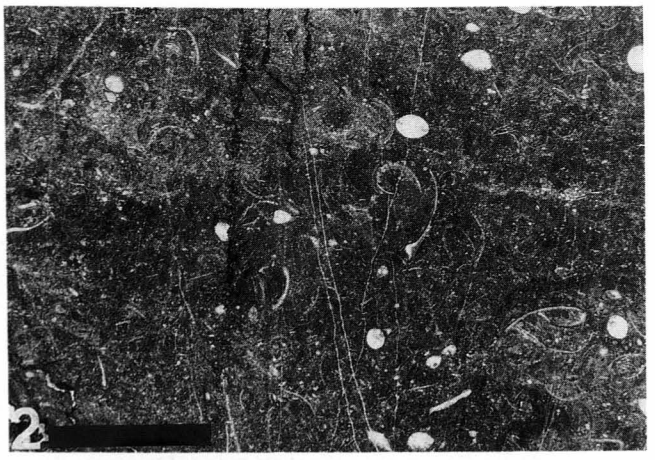
2


3

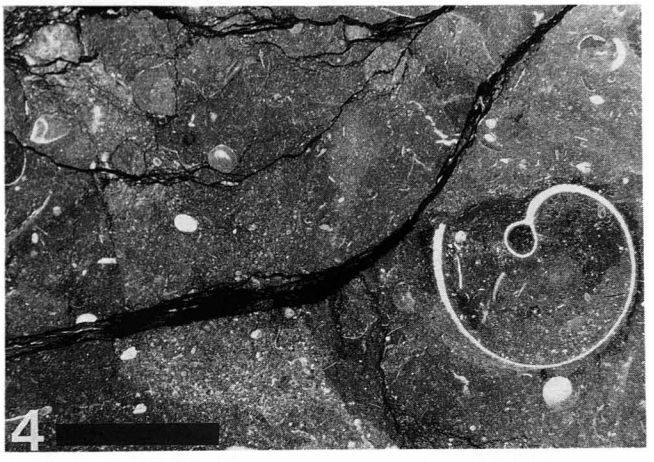
4


5

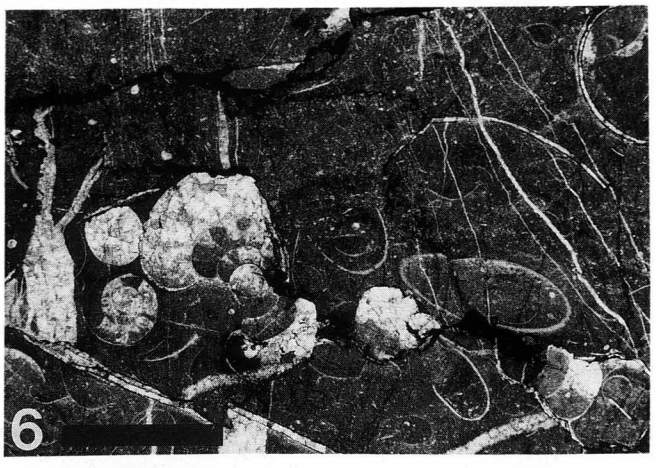
6

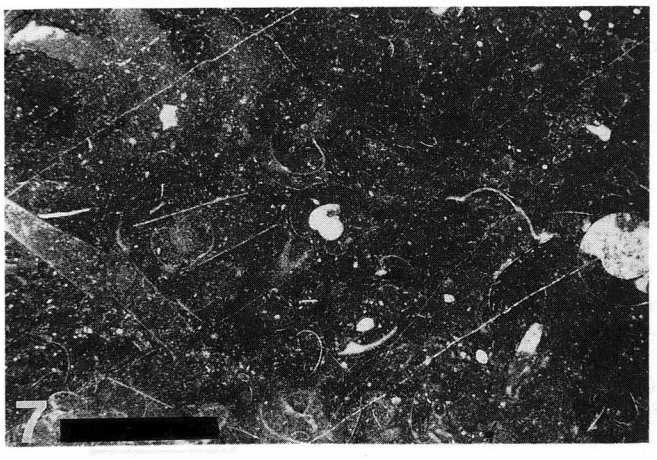
7


8

Plate 2

Microfacies of the D/C boundary beds at the Kronhofgraben section (K. BOECKELMANN).

Fig. 1: **Bioclastic wackestone (biomicrite) with ostracodes and shell fragments of molluscs.**
Thin vertical fissures.
Sample K 1, Middle (?) praesulcata Zone, late Famennian.
Scale: 1.6mm.

Fig. 2: **Bioclastic wackestone (biomicrite) with a trilobite fragment (center left) and shell fragments of molluscs.**
Numerous vertical fissures and horizontal stylolites. Broad vertical fissure at the left is filled with coarse-grained calcite.
Sample K 1, Middle (?) praesulcata Zone, late Famennian.
Scale: 1.7 mm.

Fig. 3: **Bioclastic wackestone (biomicrite) with a trilobite and shell fragments of molluscs.**
Sample K 13, sulcata Zone, early Tournaisian.
Scale: 1.6mm.

Fig. 4: **Bioclastic wackestone (biomicrite) with a coral (?) and fragments of trilobites and molluscs.**
Stylolitic seams are oriented parallel to the bedding plane.
Sample K 14, duplicata Zone, early Tournaisian.
Scale: 3.8 mm.

Fig. 5: **Bioclastic wackestone (biomicrite) with a cephalopod shell.**
Thin vertical fissures. A broad fissure on the left is filled with coarse-grained calcite.
Sample K 14, duplicata Zone, early Tournaisian.
Scale: 1.3 mm.

Fig. 6: **Bioclastic wackestone (biomicrite) with a trilobite fragment, an ostracode (center left) and shells of bivalves.**
Sample K 14, duplicata Zone, early Tournaisian.
Scale: 1.3 mm.

Fig. 7: **Bioclastic wackestone (biomicrite) with an ostracode and fine-grained biodebris.**
Sample K 14, duplicata Zone, early Tournaisian.
Scale: 1.6mm.

Fig. 8: **Mudstone (biomicrite) with a large cephalopod.**
Sample K 16, duplicata Zone, early Tournaisian.
Scale: 4 mm.

Fig. 9: **Left: bioclastic wacke and packstone (see Fig. 10).**
Right: broad fissure filled with coarse-grained calcite and angular clasts of micritic material.
Sample K 19, sandbergi Zone, early to middle Tournaisian.
Scale: 3.8 mm.

Fig. 10: **Bioclastic packstone with fragments of a conodont (center) and an echinoderm.**
Sample K 19, sandbergi Zone, early to middle Tournaisian.
Scale: 0.75 mm.

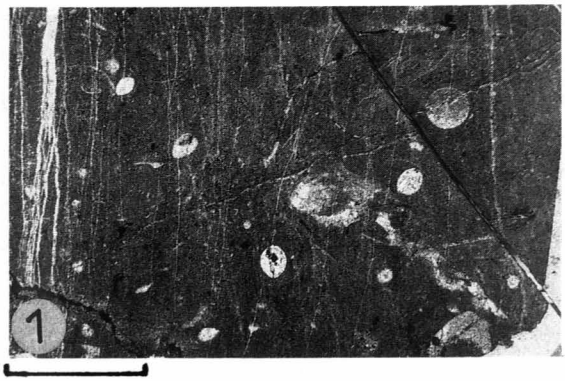
1


2

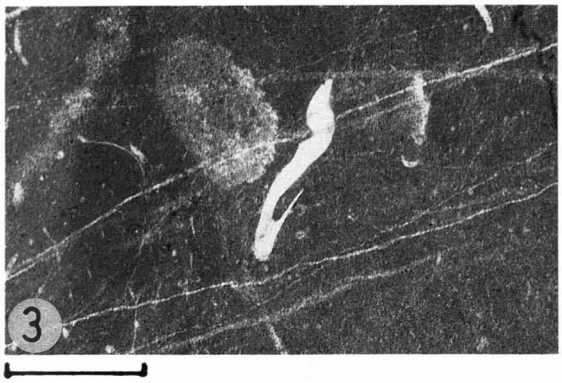
3

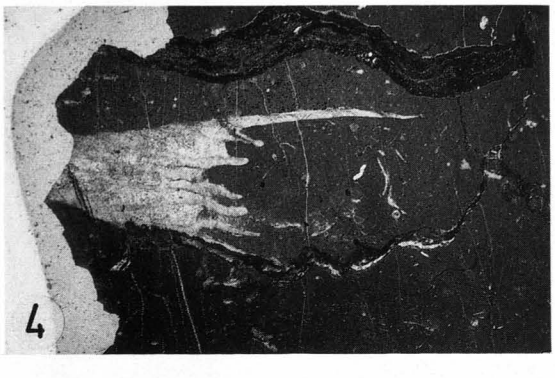
4

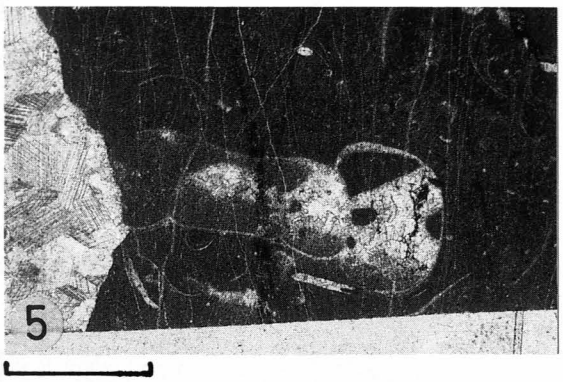
5


6

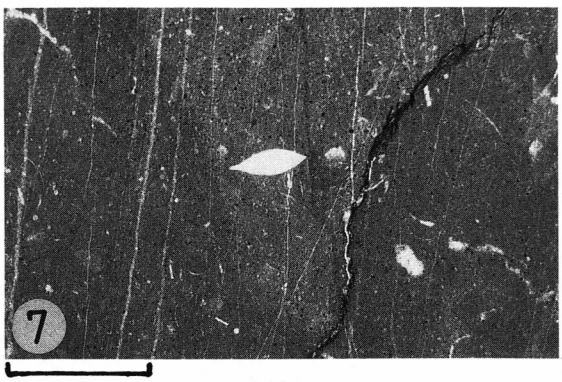
7

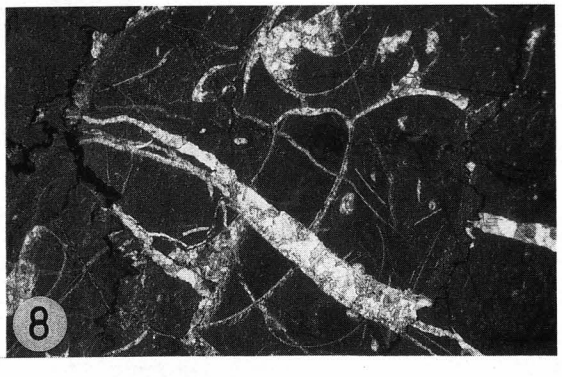
8

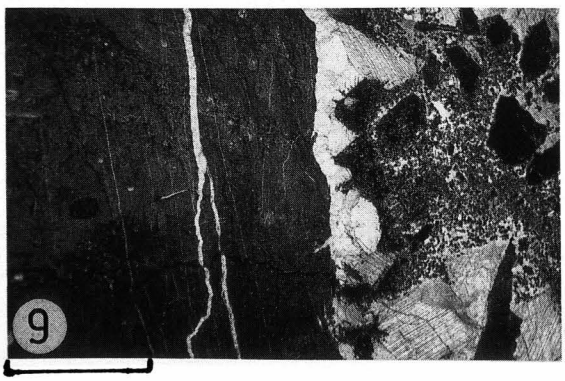
9


10

Plate 3

Conodonts from the D/C boundary beds at the Grüne Schneid (Figs. 1–17) and Kronhofgraben sections (Figs. 18–24).
For palmatolepid and protognathodid conodonts see H.P. SCHÖNLAUB et al. (1988).

Figs. 1–2: ***Polygnathus communis communis* BRANSON & MEHL.**
Both specimens display a large basal cavity.
Fig. 1: Juvenile specimen.
Grüne Schneid, sample 6 C, ×75.
Fig. 2: Grüne Schneid, sample 6 B2, ×55.

Figs. 3–7,16: ***Siphonodella sulcata* (HUDDLE).**
Figs. 3–5: Grüne Schneid, sample 6 D, ×38, ×32, ×38.
Figs. 6–7: Grüne Schneid, sample 5 B, ×31, ×42.
Fig. 16: Transitional form to *S. duplicata* MT 1, Grüne Schneid, sample 5 A, ×35.

Figs. 8–9: ***Siphonodella praesulcata* SANDBERG.**
Grüne Schneid, sample 5 C, ×30, ×39.

Figs. 10–13: ***Polygnathus mehli* THOMPSON.**
Figs. 10,12,13: Grüne Schneid, sample 5 C, ×28, ×32, ×32.
Fig. 11: Grüne Schneid, sample 5 B, ×25.

Figs. 14,15,17: ***Siphonodella duplicata* (BRANSON & MEHL), Morphotype 1.**
Figs. 14,15: Grüne Schneid, sample 5 B, ×34, ×54.
Fig. 17: Grüne Schneid, sample 5 C, ×32.

Figs. 18,19,21: ***Siphonodella sulcata* (HUDDLE).**
Figs. 18,19: Kronhofgraben, sample 14, ×31, ×31.
Fig. 21: Kronhofgraben, sample 15, ×32.

Figs. 20,23: ***Siphonodella duplicata* (BRANSON & MEHL), Morphotype 1.**
Fig. 20: Kronhofgraben, sample 15, ×53.
Fig. 23: Kronhofgraben, sample 14, ×44.

Figs. 22,24: ***Siphonodella duplicata* (BRANSON & MEHL), Morphotype 2.**
Kronhofgraben, sample 14, ×25, ×31.


1
2
3
4
5
6
7
8
9
10
11
12
13
14
15
16
17
18
19
20
21
22
23
24

Plate 4

Ammonoidea from the Devonian/Carboniferous boundary section at Grüne Schneid (see Tafel 1 in D. KORN, same volume).

Figs. 1, 2: ***Parawocklumeria paradoxa*** **(WEDEKIND 1918).**
Bed 8; ×1,8.

Fig. 3: ***Wocklumeria sphaeroides*** **(REINH. RICHTER 1848).**
Bed 8; ×1,8.

Figs. 4, 5: ***Cymaclymenia striata*** **(MÜNSTER 1832).**
Bed 8; ×0,9.

Figs. 6, 7: ***Linguaclymenia similis*** **(MÜNSTER 1839).**
Bed 6A; ×1,2.

Figs. 8: ***Cymaclymenia striata*** **(MÜNSTER 1832).**
Bed 6A; ×0,6.

Fig. 9: ***Finiclymenia wocklumensis*** **LANGE 1929.**
Bed 6A; ×1,8.

Figs. 10,11: ***Acutimitoceras carinatum*** **(H. SCHMIDT 1924).**
Bed 6B; ×1,4.

Figs. 12,13: ***Acutimitoceras carinatum*** **(H. SCHMIDT 1924).**
Bed 6B; ×0,7.

Fig. 14: ***Acutimitoceras*** **cf.** ***prorsum*** **(H. SCHMIDT 1925),** ***Acutimitoceras*** **cf.** ***kleinerae*** **KORN 1984.**
Bed 6C; ×1,8.

Figs. 15,16: ***Acutimitoceras*** **cf.** ***intermedium*** **(SCHINDEWOLF 1923).**
Bed 6C; ×1,8.

Figs. 17,18: ***Gattendorfia subinvoluta*** **(MÜNSTER 1832).**
Bed 6D; ×1,8.

Figs. 19,20: ***Acutimitoceras acutum*** **(SCHINDEWOLF 1923).**
Bed 6D; ×0,7.

Fig. 21: ***Imitoceras*** **sp..**
Bed 6D; ×1,2.

Figs. 22,23: ***Acutimitoceras intermedium*** **(SCHINDEWOLF 1923).**
Bed 6D; ×0,9.

Figs. 24,25: ***Acutimitoceras intermedium*** **(SCHINDEWOLF 1923).**
Bed 6D; ×1,4.

Figs. 26,27: ***Acutimitoceras intermedium*** **(SCHINDEWOLF 1923).**
Bed 6D; ×1,8.

Figs. 28,29: ***Acutimitoceras subbilobatum*** **(MÜNSTER 1839).**
Bed 6D; ×1,8.

Fig. 30: ***Acutimitoceras intermedium*** **(SCHINDEWOLF 1923).**
Bed 6D; ×1,8.

All specimen coll. KORN 1988, stored under inventory numbers 89/1/1–18 in the Geologische Bundesanstalt in Vienna.

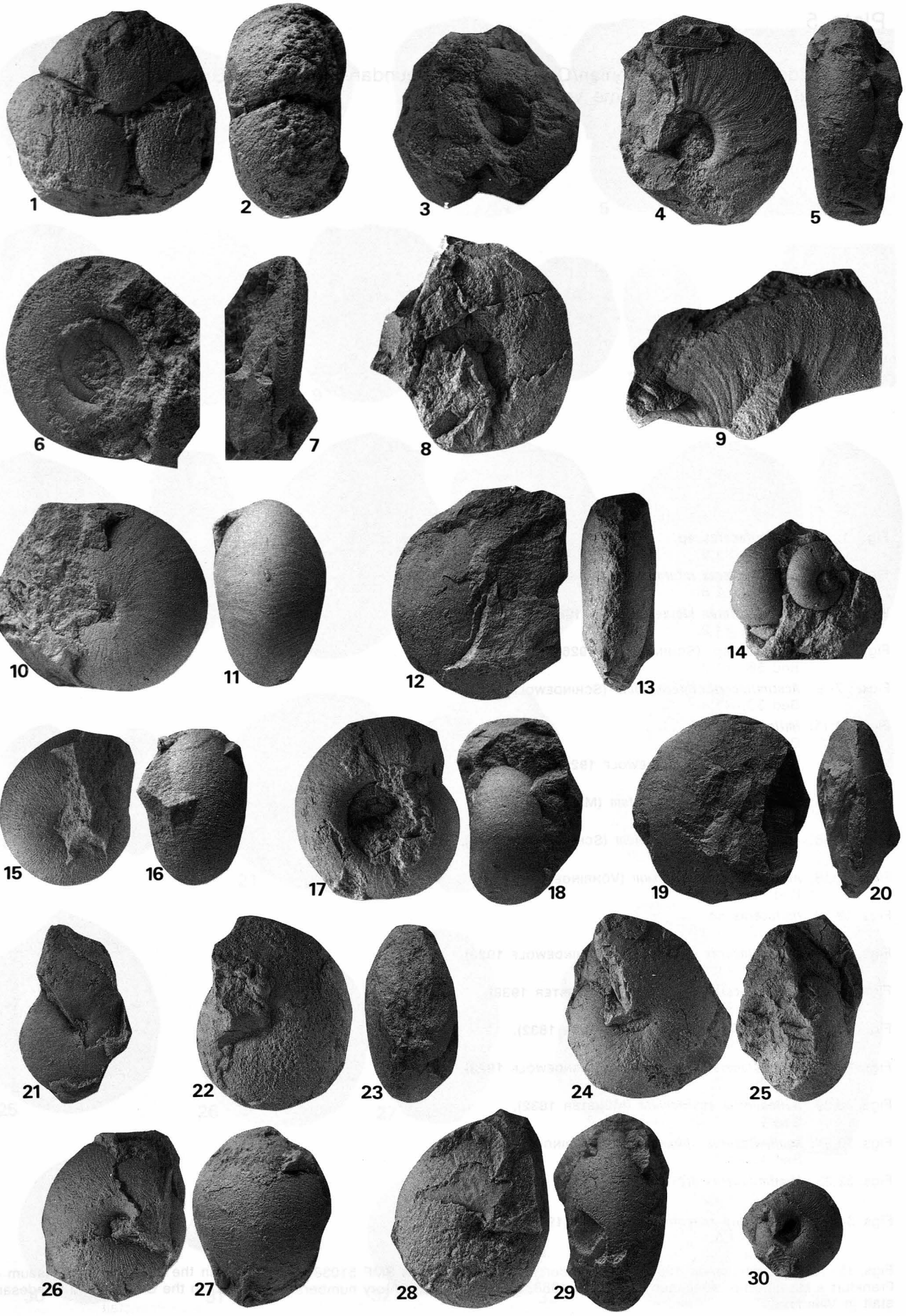
1
2
3
4
5
6
7
8
9
10
11
12
13
14
15
16
17
18
19
20
21
22
23
24
25
26
27
28
29
30

Plate 5

Ammonoidea from the Devonian/Carboniferous boundary section at Grüne Schneid (see Tafel 2 in D. KORN, same volume).

Fig. 1: ***Acutimitoceras* sp.**
Bed 5A; ×1,8.

Figs. 2, 3: ***Acutimitoceras intermedium* (SCHINDEWOLF 1923).**
Bed 5A; ×1,8.

Figs. 4, 5: ***Acutimitoceras kleinerae* KORN 1984.**
Bed 5B; ×1,2.

Fig. 6: ***Eocanites* sp. (SCHINDEWOLF 1926).**
Bed 5B; ×1,2.

Figs. 7–9: ***Acutimitoceras intermedium* (SCHINDEWOLF 1923).**
Bed 5B; ×1,4.

Figs. 10,11: ***Imitoceras* sp..**
Bed 5B; ×1,8.

Figs. 12: ***Eocanites* sp. (SCHINDEWOLF 1926).**
Bed 5B; ×1,8.

Figs. 13,14: ***Acutimitoceras subbilobatum* (MÜNSTER 1839).**
Bed 5C; ×0,9.

Figs. 15,16: ***Acutimitoceras intermedium* (SCHINDEWOLF 1923).**
Bed 5C; ×0,7.

Figs. 17,18: ***Acutimitoceras convexum* (VÖHRINGER 1960).**
Bed 5C; ×1,4.

Figs. 19,20: ***Imitoceras* sp..**
Bed 5D; ×1,8.

Figs. 21,22: ***Acutimitoceras intermedium* (SCHINDEWOLF 1923).**
Bed 3A; ×1,4.

Figs. 23,24: ***Acutimitoceras subbilobatum* (MÜNSTER 1939).**
Bed 3A; ×1,8.

Fig. 25: ***Gattendorfia subinvoluta* (MÜNSTER 1832).**
Bed 3B; ×1,4

Figs. 26,27: ***Acutimitoceras intermedium* (SCHINDEWOLF 1923).**
Bed 2; ×1,2.

Figs. 28,29: ***Gattendorfia subinvoluta* (MÜNSTER 1832).**
Bed 2; ×1,2.

Figs. 30,31: ***Acutimitoceras sphaeroidale* (VÖHRINGER 1960).**
Bed 1; ×1,8.

Figs. 32,33: ***Mimimitoceras crestaverde* n.sp.**
Bed 1; ×1,8.

Figs. 34,35: ***Gattendorfia reticulum* VÖHRINGER 1960.**
Bed 1; ×1,8.

Figs. 15–18 coll. SCHÖNLAUB 1986, stored under catalogue numbers SMF 51038 resp. 51036 in the Senckenberg Museum in Frankfurt a.M.; all other specimen coll. KORN 1988, stored under inventory numbers 89/1/19–37 in the Geologische Bundesanstalt in Vienna.


1
2
3
4
5
6
7
8
9
10
11
12
13
14
15
16
17
18
19
20
21
22
23
24
25
26
27
28
29
30
31
32
33
34
35

Plate 6

For detailed explanation see Tafel 1 in R. FEIST (same volume).

Fig. 1,3–5,7: ***Helioproetus carintiacus*** **(DREVERMANN, 1901).**
Fig. 1: Grüne Schneid: Bed 13, ×8,1.
Fig. 3: Grüne Schneid: Bed 6A.
a) Oral view; ×8,2.
b) Lateral view; ×8,1.
Fig. 4: Bed 8; ×9,7.
Fig. 5: Grüne Schneid: Bed 8.
a) Oral view; ×6,2.
b) Lateral view; ×6,2.
Fig. 7: Grüne Schneid: Bed 8.
a) Oral view; ×7,4.
b) Lateral view; ×6,2.
c) Posterior view; ×6,6.

Fig. 2,8–9: ***Helioproetus subcarintiacus*** **(RUD. RICHTER, 1913).**
Fig. 2: Grüne Schneid: Bed 15, ×7,4.
Fig. 8: Grüne Schneid: Bed 8.
a) Oral view; ×6,7.
b) Lateral view; ×6,2.
Fig. 9: Grüne Schneid: Bed 9, ×7,5.

Fig. 6: ***Helioproetus*** **cf.** ***ebersdorfensis*** **(RUD. RICHTER, 1913).**
Grüne Schneid: Bed 9.
a) Oral view; ×9,3.
b) Posterior view; ×6,5.

Fig. 10: ***Phacops (Phacops) granulatus*** **(MÜNSTER, 1840).**
Grüne Schneid: Bed 9.
a) Oral view; ×6.
b) Lateral view; ×6.

Fig. 11: ***Typhloproetus (Silesiops)*** **sp.**
Grüne Schneid: Bed 9, ×6,8.

Fig. 12–18: ***Typhloproetus (Silesiops) korni*** **n.sp.**
Fig. 12: Grüne Schneid: Bed 9.
a) Oral view; ×11,4.
b) Lateral view; ×10,6.
Fig. 13: Grüne Schneid: Bed 13, ×8,2.
Fig. 14: Grüne Schneid: Bed 9, ×9.
Fig. 15: Grüne Schneid: Bed 13, ×11,9.
Fig. 16: Grüne Schneid: Bed 8.
a) Oral view; ×7,8.
b) Oblique lateral view; ×9,7.
Fig. 17: Grüne Schneid: Bed 8, ×8,8.
Fig. 18: Grüne Schneid: Bed 9.
a) Oral view; ×8,1.
b) Lateral view; ×6,3.

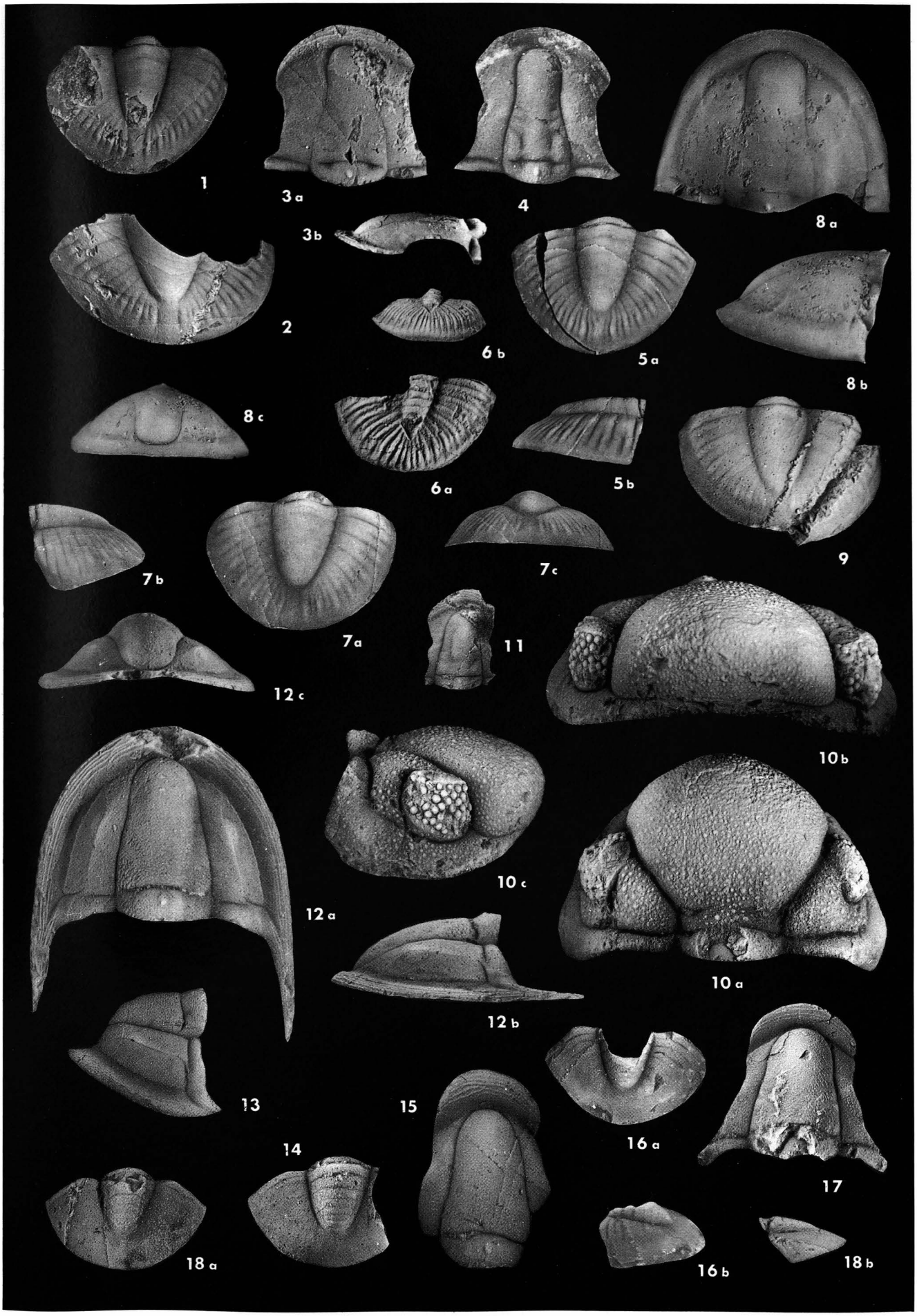
1
3a
4
8a
3b
2
6b
5a
8b
8c
6a
5b
9
7b
7a
7c
11
12c
10b
10c
12a
10a
12b
13
15
16a
17
14
18a
16b
18b

Plate 7

For detailed explanation see Tafel 2 in R. FEIST (same volume).

Fig. 1– 6: ***Belgibole abruptirhachis*** **(RUD. & E. RICHTER, 1951).**
- Fig. 1: Grüne Schneid: Bed 6B, ×8,8.
- Fig. 2: Grüne Schneid: Bed 6B.
  - a) Oral view; ×6,4.
  - b) Lateral view; ×6,5.
- Fig. 3: Grüne Schneid: Bed 6B, ×6,0.
- Fig. 4: Grüne Schneid: Bed 6B.
  - a) Oral view; ×7,1.
  - b) Lateral view; ×8,2.
- Fig. 5: Grüne Schneid: Bed 6B.
  - a) Oral view; ×6.
  - b) Posterior view; ×6,5.
- Fig. 6: Grüne Schneid: Bed 6B, ×6,9.

Fig. 7– 9: ***Semiproetus (Macrobole)*** **cf.** ***funirepa*** **(FEIST, 1988).**
- Fig. 7: Grüne Schneid: Bed 6C.
  - a) Oral view; ×5,7.
  - b) Lateral view; ×5,9.
- Fig. 8: Grüne Schneid: Bed 6C, ×8,1.
- Fig. 9: Grüne Schneid: Bed 6B (upper part).
  - a) Oral view; ×5,3.
  - b) Lateral view; ×6,2.

Fig. 10–14: ***Liobolina submonstrans*** **RUD. & E. RICHTER, 1951.**
- Fig. 10: Grüne Schneid: Bed 5B.
  - a) Oral view; ×3,9.
  - b) Posterior view; ×3,6.
- Fig. 11: Grüne Schneid: Bed 5B.
  - a) Oral view; ×5,9.
  - b) Lateral view; ×5,7.
- Fig. 12: Grüne Schneid: Bed 2.
  - a) Oral view; ×6,8.
  - b) Posterior view; ×8,4.
- Fig. 13: Grüne Schneid: Bed 5C.
  - a) Oral view; ×4,6.
  - b) Posterior view; ×4,5.
- Fig. 14: Grüne Schneid: Bed 5B.
  - a) Oral view; ×7,2.
  - a) Lateral view; ×6,7.
  - c) Posterior view; ×7,2.

Fig. 15–19: ***Liobolina crestaverdensis*** **n.sp.**
- Fig. 15: Grüne Schneid: Bed 6D.
  - a) Oral view; ×5,2.
  - b) Lateral view; ×5,6.
  - c) Anterior view; ×5,6.
- Fig. 16: Grüne Schneid: Bed 6D.
  - a) Oral view; ×6,6.
  - b) Lateral view; ×6,1.
- Fig. 17: Grüne Schneid: Bed 6D.
  - a) Oral view; ×4,5.
  - b) Lateral view; ×3,7.
- Fig. 18: Grüne Schneid: Bed 6D.
  - a) Oral view; ×4,5.
  - b) Posterior view; ×5,9.
- Fig. 19: Grüne Schneid: Bed 6D.
  - a) Oral view; ×4,5.
  - b) Lateral view; ×4,5.

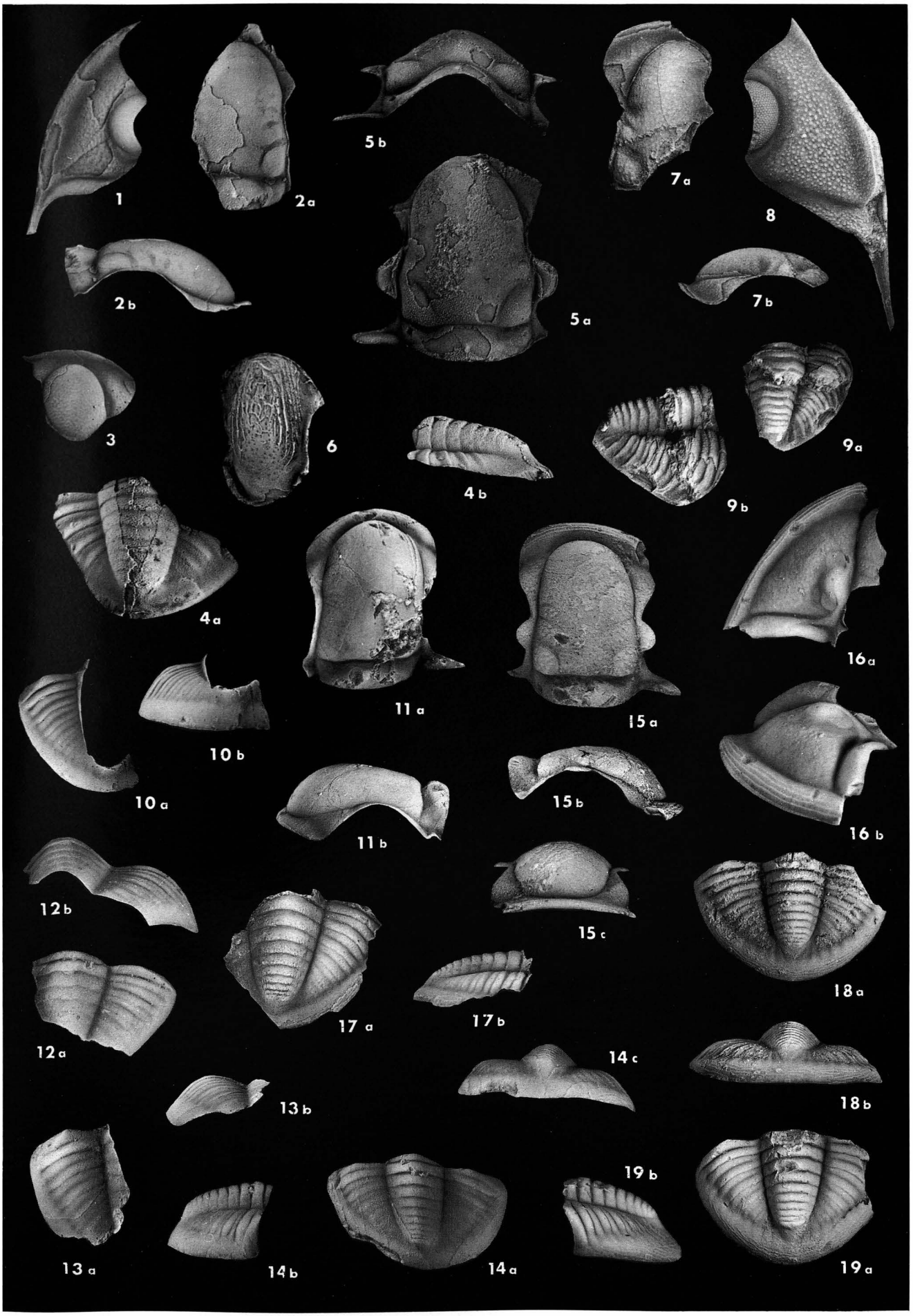
1
2a
2b
5b
5a
7a
8
7b
3
6
4b
9a
9b
4a
11a
15a
16a
10b
10a
11b
15b
16b
12b
15c
18a
12a
17a
17b
14c
18b
13b
13a
14b
14a
19b
19a

Plate 8

For detailed explanation see Tafel 3 in R. FEIST (same volume).

Fig. 1–9,14–17: ***Semiproetus (Macrobole) hercules*** **(RUD. & E.RICHTER, 1951).**

Fig. 1: Grüne Schneid: Bed 6D.
a) Oral view; ×7,3.
b) Lateral view; ×7,2.

Fig. 2: Grüne Schneid: Bed 5B.
a) Oral view; ×6,5.
b) Anterior view; ×4,9.
c) Lateral view; ×5,8.

Fig. 3: Grüne Schneid: Bed 5A.
a) Oral view; ×6,3.
b) Lateral view; ×6,1.

Fig. 4: Grüne Schneid: Bed 5B, ×6,1.
Fig. 5: Grüne Schneid: Bed 5B, ×5,3.

Fig. 6: Grüne Schneid: Bed 5B.
a) Oral view; ×8,1.
b) Lateral view; ×6,2.

Fig. 7: Grüne Schneid: Bed 5B.
a) Oral view; ×5,3.
b) Lateral view; ×5,4.

Fig. 8: Grüne Schneid: Bed 5A, ×7,5.
Fig. 9: Grüne Schneid, Bed 5A, ×8,4.
Fig. 14: Grüne Schneid: Bed 6D,×4,7.
Fig. 15: Grüne Schneid: Bed 5B, ×7,3.
Fig. 16: Grüne Schneid: Bed 5B, ×5.

Fig. 17: Grüne Schneid: Bed 5B.
a) Oral view; ×7,3.
b) Lateral view; ×6,3.

Fig. 10: ***Semiproetus (Macrobole)*** **sp. aff.** ***drewerensis*** **(RUD. & E. RICHTER, 1951).**
Grüne Schneid: Bed 5B.
a) Oral view; ×7,1.
b) Posterior view; ×7,0.

Fig. 11–13: ***Cyrtoproetus (Cyrtoproetus) blax*** **(RUD. & E. RICHTER, 1951).**

Fig. 11: Grüne Schneid: Bed 2.
a) Oral view; ×7,2.
b) Lateral view; ×6,6.

Fig. 12: Grüne Schneid: Bed 3.
a) Oral view; ×5,5.
b) Lateral view; ×5,4.

Fig. 13: Grüne Schneid: Bed 2.
a) Oral view; ×4,8.
b) Lateral view; ×4,8.

Fig. 18–19: ***Semiproetus (Macrobole) drewerensis*** **(RUD. & E. RICHTER, 1951).**

Fig. 18: Grüne Schneid: Bed 2, ×9,1.

Fig. 19: Grüne Schneid: Bed 2.
a) Oral view; ×5,8.
b) Lateral view; ×6,0.

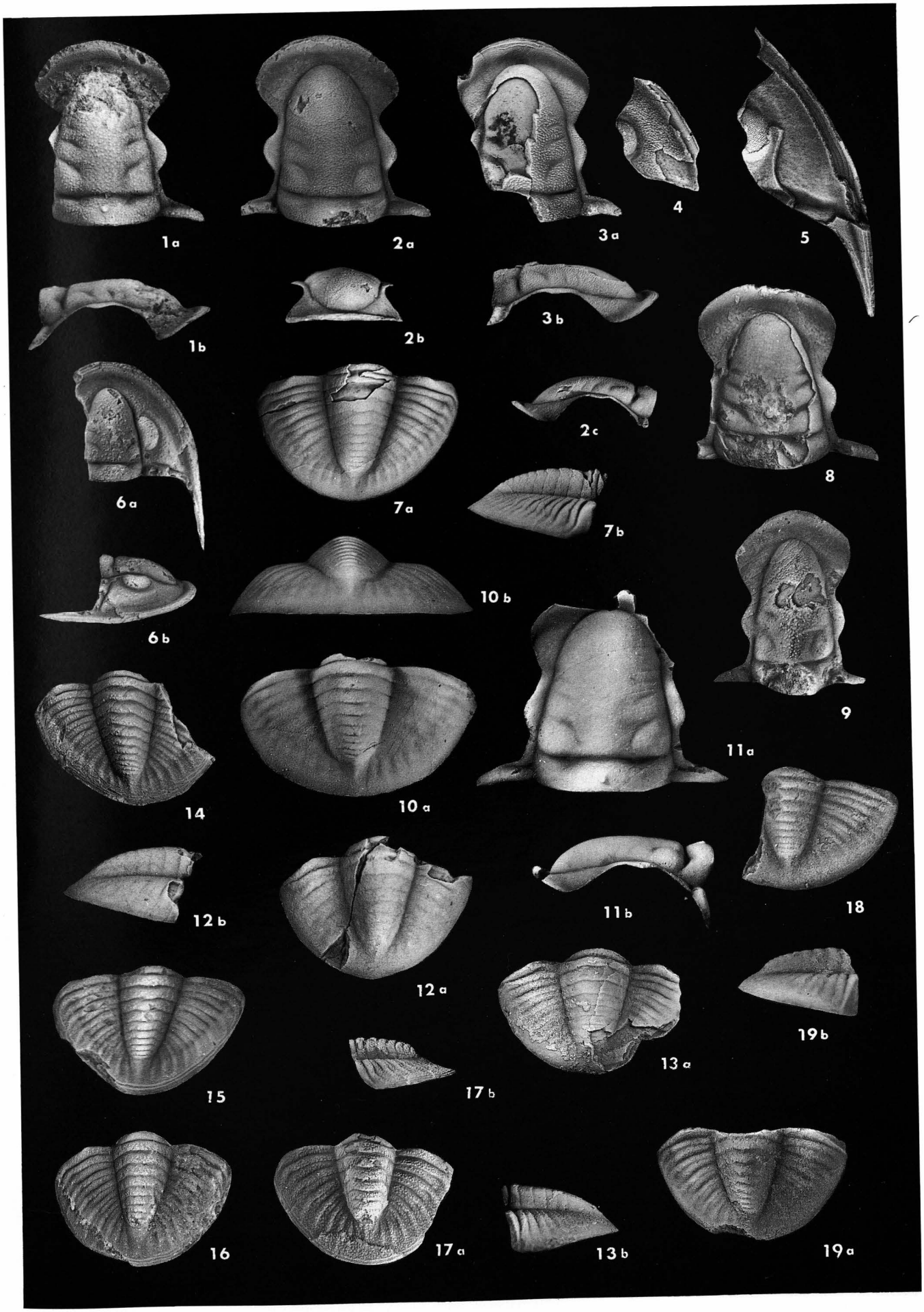
1a
2a
3a
4
5
1b
2b
3b
2c
8
6a
7a
7b
6b
10b
9
11a
14
10a
18
12b
11b
12a
19b
15
17b
13a
16
17a
13b
19a

Plate 9

For detailed explanation see Tafel 4 in R. FEIST (same volume).

Fig. 1– 2: ***Chaunoproetus (Chaunoproetus) carnicus*** **(RUD. RICHTER, 1913).**
Fig. 1: Grüne Schneid: Bed 12, ×10,7.
Fig. 2: Grüne Schneid: Bed 12.
a) Oral view; ×11,7.
b) Lateral view; ×8,9.

Fig. 3– 4: ***Chaunoproetus (Chaunoproetus)*** **cf.** ***palensis*** **(RUD. RICHTER, 1913).**
Fig. 3: Grüne Schneid: Bed 6A, ×3,3.
Fig. 4: Grüne Schneid: Bed 6A.
a) Oral view; ×6,6.
b) Lateral view; ×5,5.

Fig. 5– 6: ***Haasia*** **cf.** ***antedistans*** **(RUD. & E. RICHTER, 1926).**
Fig. 5: Grüne Schneid: Bed 12, ×11,8.
Fig. 6: Grüne Schneid: Bed 9, ×8,9.

Fig. 7–10: ***Semiproetus (Macrobole) brevis*** **n.sp.**
Fig. 7: Grüne Schneid: Bed 3, ×7,4.
Fig. 8: Grüne Schneid: Bed 2, ×9,1.
Fig. 9: Grüne Schneid: Bed 2, ×9,1.
Fig. 10: Grüne Schneid: Bed 1, ×8,1.

Fig. 11,19–20: ***Diacoryphe schoenlaubi*** **n.sp.**
Fig. 11: Grüne Schneid: Bed 1.
a) Oral view; ×7,3.
b) Lateral view; ×7,1.
Fig. 19: Grüne Schneid: Bed 1, ×8,3.
Fig. 20: Grüne Schneid: Bed 1.
a) Oral view; ×7,8.
b) Lateral view; ×7,8.

Fig. 12–14,21: ***Archegonus (Phillibole?) planus*** **n.sp.**
Fig. 12: Grüne Schneid: Bed 1, ×5,4.
Fig. 13: Grüne Schneid: Bed 1.
a) Oral view; ×7,2.
b) Lateral view; ×7,1.
c) Anterior view; ×6,2.
Fig. 14: Grüne Schneid: Bed 1, ×7,5.
Fig. 21: Grüne Schneid: Bed 1, ×4,7.

Fig. 15–17,?18: ***Phillibolоides macromma*** **n.sp.**
Fig. 15: Grüne Schneid: Bed 1, ×5.
Fig. 16: Grüne Schneid: Bed 3, ×8,1.
Fig. 17: Grüne Schneid: Bed 1, ×4,2.
Fig. 18: Grüne Schneid: Bed 1.
a) Oral view; ×6,8.
b) Lateral view; ×6,6.

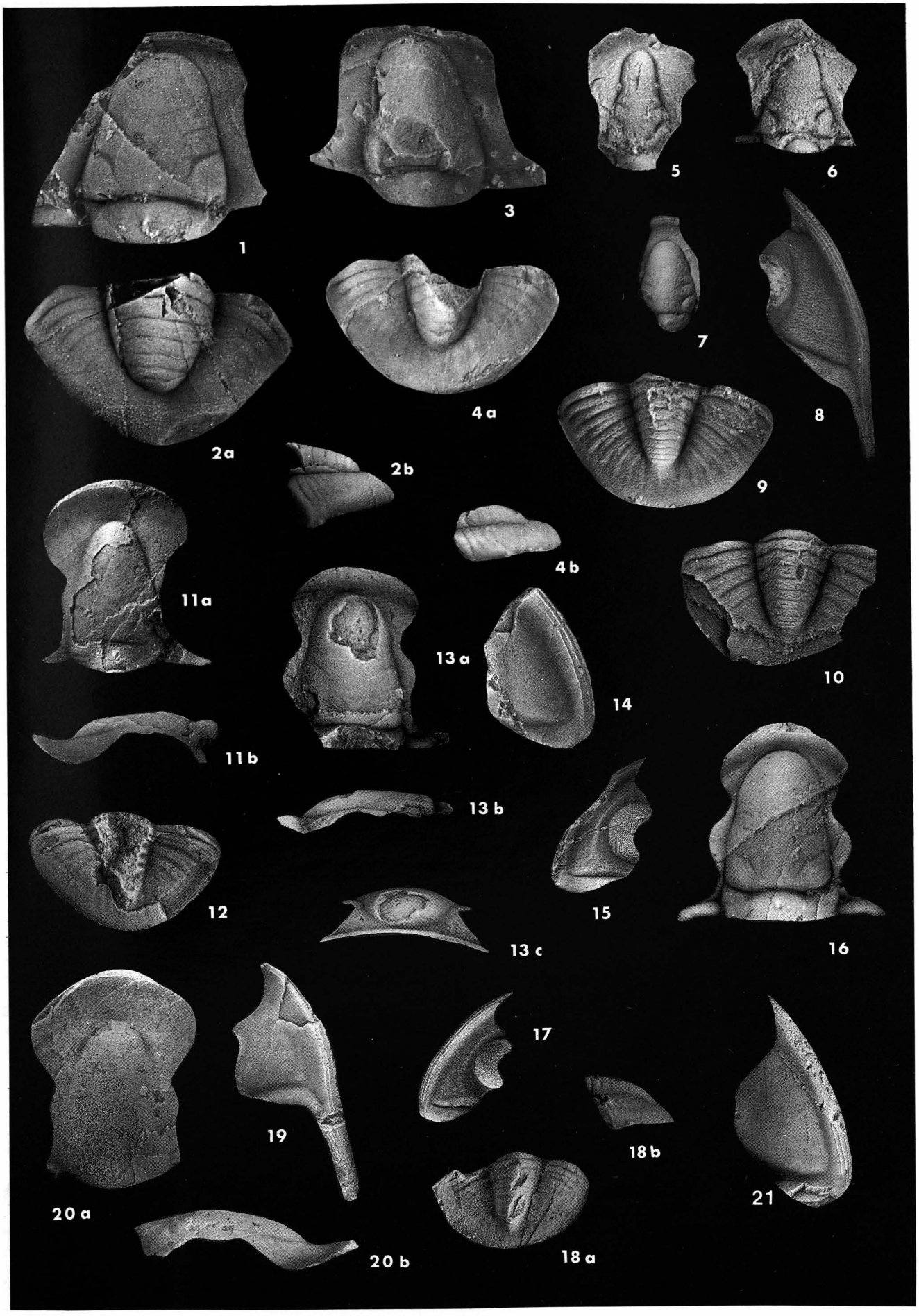
1
3
5
6
2a
4a
7
8
2b
9
4b
11a
13a
10
14
11b
13b
12
15
16
13c
17
19
18b
21
20a
18a
20b

References

ANDERSON, T.F. (1990): Temperature from Oxygen Isotope Ratios. – In: D.E.G. BRIGGS & P.R. CROWTHER (Eds.): Palaeobiology. A synthesis. – 403–406, Oxford – Melbourne (Blackwell Sc. Publ.).

ATTREP, M., Jr., ORTH, C.J. & QUINTANA, L.R. (1991): The Permian-Triassic of the Gartnerkofel-1 Core (Carnic Alps, Austria): Geochemistry of Common and Trace Elements II–INAA and RNAA. – In: W.T. HOLSER & H.P. SCHÖNLAUB (Eds.): The Permian-Triassic Boundary in the Carnic Alps of Austria (Gartnerkofel Region). – Abh. Geol. B.-A., **45**, 123–137, Wien.

COWIE, J.W., ZIEGLER, W., BOUCOT, A.J., BASSETT, M.G. & REMANE, J. (1986): Guidelines and Statues of the International Commission on Stratigraphy (ICS). – Cour. Forsch.-Inst. Senckenberg, **83**, 1–14, Frankfurt.

DYER, B.D., LYALIKOVA, N.N., MURRAY, D., DOYLE, M., KOLESOV, G.M. & KRUMBEIN, W. E. (1989): Role of microorganisms in the formation of iridium anomalies. – Geology, **17**, 1036–1039, Boulder.

EBNER, F. (1973): Die Conodontenfauna des Devon/Karbon-Grenzbereiches am Elferspitz (Karnische Alpen, Österreich). – Mitt. Abt. Geol. Paläont. Bergb. Landesmus. Joanneum, **34**, 3–24, Graz.

FLAJS, G., FEIST, R. & ZIEGLER, W. (Eds.) (1988): Devonian-Carboniferous Boundary – Results of recent studies. – Cour. Forsch.-Inst. Senckenberg, **100**, 1–245.

FREY, M. (Ed.) (1987): Low Temperature Metamorphism. – 1–351, Blackie, Glasgow.

GAERTNER, H.R. von (1931): Geologie der zentralkarnischen Alpen. – Denkschr. Österr. Akad. Wiss., math.-naturw. Kl., **102**, 113–199, Wien.

HAHN, G. & KRATZ, R. (1992): Eine Trilobiten-Fauna des tiefen Wassers aus dem Unter-Karbon der Karnischen Alpen (Österreich) – vorläufige Mitteilung. – Jb. Geol. B.-A., **135**/1, Wien.

HSÜ, K.J. & MCKENZIE, J.A. (1985): A "Strangelove" ocean in the earliest Tertiary. – In: E.T. SUNDQUIST & W.S. BROECKER (Eds.): The carbon cycle and atmospheric CO_2: Natural variations Archean to present. – Amer. Geophys. Union, 487–492, Washington.

JOHNSON, J.G., KLAPPER, G. & SANDBERG, C.A. (1985): Devonian eustatic fluctuations in Euramerica. – Geol. Soc. Amer. Bull., **96**, 567–587, Boulder.

KLEIN, P. (1991): The Permian-Triassic of the Gartnerkofel-1 Core (Carnic Alps, Austria): Geochemistry of Common and Trace Elements I–ICP, AAS and LECO. – In: W.T. HOLSER & H.P. SCHÖNLAUB (Eds.): The Permian-Triassic Boundary in the Carnic Alps of Austria (Gartnerkofel Region). – Abh. Geol. B.-A., **45**, 109–121, Wien.

KORN, D. (1984): Die Goniatiten der Stockumer *Imitoceras*-Kalklinsen (Ammonoidea; Devon/Karbon-Grenze). – Cour. Forsch.-Inst. Senckenberg, **67**, 71–89, Frankfurt.

KUMP, L.R. (1991): Interpreting carbon-isotope excursions: Strangelove oceans. – Geology, **19**, 299–302, Boulder.

MAGARITZ, M. (1989): $\delta^{13}C$ minima follow extinction events: a clue to faunal radiation. – Geology, **17**, 337–340, Boulder.

MAGARITZ, M. (1991): Carbon isotopes, time boundaries and evolution. – Terra Nova, **3**, 251–256, Oxford.

MAGARITZ, M. & HOLSER, W.T. (1990): Carbon isotope shift in Pennsylvanian seas. – Amer. J. Sci., **290**, 977–994.

ORTH, C.J. (1989): Geochemistry of the Bio-Event Horizons. – In: S.K. DONOVAN (Ed.): Mass extinctions, Processes and Evidence . – 37–72, Stuttgart (Enke).

ORTH, C.J., QUINTANA, L.R., GILMORE, J.S., GRAYSON, R.C. & WESTERGAARD, E.H. (1986): Trace element anomalies at the Mississippian/Pennsylvanian boundary in Oklahoma and Texas. – Geology, **14**, 986–990, Boulder.

ORTH, C.J., QUINTANA, L.R., GILMORE, J.S., BARRICK, J.E., HAYWA, J.N. & SPESSHARDT, S.A. (1988): Pt-metal anomalies in the Lower Mississippian of southern Oklahoma. – Geology, **16**, 627–630, Boulder.

PAPROTH, E. (1980): The Devonian-Carboniferous boundary. – Lethaia, **13**, 287, Oslo.

PAPROTH, E. & STREEL, M. (Eds.) (1984): The Devonian-Carboniferous Boundary. – Cour. Forsch.-Inst. Senckenberg, **67**, 1–258, Frankfurt.

PAPROTH, E. & SEVASTOPULO, G.D. (1988): The search for a stratotype for the base of the Carboniferous. – Cour. Forsch.-Inst. Senckenberg, **100**, 1–2, Frankfurt.

POPP, B.N., ANDERSON, T.F. & SANDBERG, P.A. (1986): Brachiopods as indicators of original isotopic compositions in some Paleozoic limestones. – Bull. Geol. Soc. Amer., **97**, 1262–1269, Boulder.

SCHÖNLAUB, H.P. (1969a): Conodonten aus dem Oberdevon und Unterkarbon des Kronhofgrabens (Karnische Alpen, Österreich). – Jb. Geol. B.-A., **112**, 321–354, Wien.

SCHÖNLAUB, H.P. (1969b): Das Paläozoikum zwischen Bischofalm und Hohem Trieb (Zentrale Karnische Alpen). – Jb. Geol. B.-A., **112**, 265–320, Wien.

SCHÖNLAUB, H.P. (1985): Geologische Karte der Republik Österreich, Blatt 197 Kötschach, 1 : 50.000, Beilagen 1 : 10.000. – Wien (Geol. B.-A.).

SCHÖNLAUB, H.P., FEIST, R. & KORN, D. (1988): The Devonian-Carboniferous Boundary at the section "Grüne Schneid" (Carnic Alps, Austria): A preliminary report. – Cour. Forsch.-Inst. Senckenberg, **100**, 149–167, Frankfurt.

SCHÖNLAUB, H.P., KLEIN, P., MAGARITZ, M., RANTITSCH, G. & SCHARBERT, S. (1991): Lower Carboniferous Paleokarst in the Carnic Alps (Austria, Italy). – Facies, **25**, 91–118, Erlangen.

SCHRAMM, J.-M. (1991): The Permian-Triassic of the Gartnerkofel-1 Core (Carnic Alps, Austria): Illite Crystallinity in Shaly Sediments and its Comparison with Pre-Variscan Sequences. – In: W.T. HOLSER & H.P. SCHÖNLAUB (Eds.): The Permian-Triassic Boundary in the Carnic Alps of Austria (Gartnerkofel Region). – Abh. Geol. B.-A., **45**, 69–77, Wien.

VEIZER, J., FRITZ, P. & JONES, B. (1986): Geochemistry of brachiopods: Oxygen and Carbon isotopic records of Paleozoic oceans. – Geochim. Cosmochim. Acta, **50**, 1679–1696, New York.

WALLACE, M.W., GOSTIN, V.A. & KEAYS, R.R. (1990): The Acraman impact ejecta and host shales: Evidence for low-temperature mobilization of iridium and other platinoids. – Geology, **18**, 132–135, Boulder.

WALLACE, M.W., KEAYS, R.R. & GOSTIN, V.A. (1991): Stromatolitic iron oxides: Evidence that sea-level changes can cause sedimentary iridium anomalies. – Geology, **19**, 551–554, Boulder.

WALLISER, O.H. (1984): Pleading for a natural D/C Boundary. – Cour. Forsch.-Inst. Senckenberg, **67**, 241–246, Frankfurt.

YOUNG, G. & CLAOUÉ-LONG, J. (1991): Age control on sedimentary sequences. – BMR Res. Newsletter, **15**, 14–16, Canberra.

YU, C.M. (Ed.) (1988): Devonian-Carboniferous Boundary in Nanbiancun, Guilin, China – Aspects and Records. – 1–379, Beijing (Science Press).

ZIEGLER, W. & SANDBERG, C.A. (1984): *Palmatolepis*-based revision of upper part of standard Late Devonian conodont zonation. – Geol. Soc. Amer. Spec. Pap., **196**, 179–194, Boulder.